Article

Isotopic Probing of Molecular Oxygen Activation at Copper(I) Sites

Michael P. Lanci, Valeriy V. Smirnov, Christopher J. Cramer,
Ekaterina V. Gauchenova, Jrg Sundermeyer, and Justine P. Roth

J. Am. Chem. Soc., **2007**, 129 (47), 14697-14709 • DOI: 10.1021/ja074620c

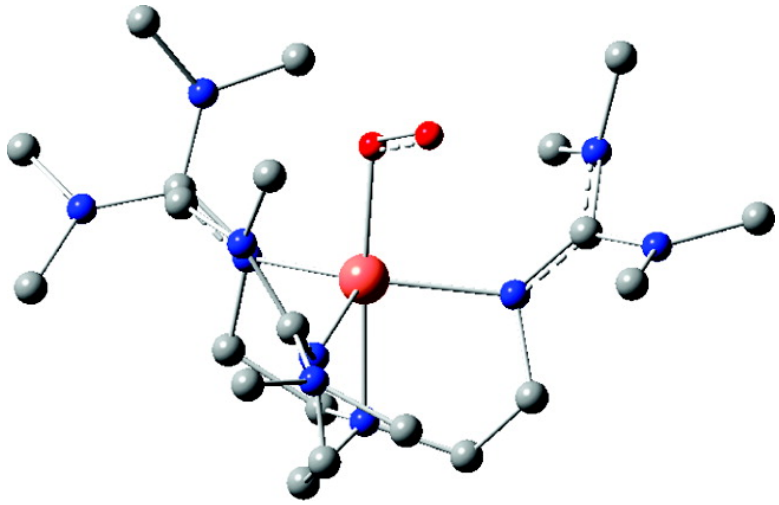

J|A|C|S
ARTICLES
Published on Web 10/26/2007

Isotopic Probing of Molecular Oxygen Activation at Copper(I) Sites

Michael P. Lanci,[†] Valeriy V. Smirnov,[†] Christopher J. Cramer,[‡] Ekaterina V. Gauchenova,[§] Jörg Sundermeyer,[§] and Justine P. Roth*,[†]

Contribution from the Department of Chemistry, Johns Hopkins University, 3400 North Charles Street, Baltimore, Maryland 21218, Department of Chemistry, Supercomputer Institute and Center for Metals in Biocatalysis, University of Minnesota, 207 Pleasant Street Southeast, Minneapolis, Minnesota 55410, and Fachbereich Chemie, Philipps-Universität Marburg, Hans-Meerwein-Strasse, 35032 Marburg, Germany

Received June 24, 2007; E-mail: jproth@jhu.edu

Abstract: Copper−dioxygen (CuO_2) adducts are frequently proposed as intermediates in enzymes, yet their electronic and vibrational structures have not always been understood. [Cu(η^1-O_2)TMG_3tren]$^+$ (TMG_3-tren = 1,1,1-tris{2-[N^2-(1,1,3,3-tetramethylguanidino)]ethyl}amine) features end-on (η^1) O_2 coordination in the solid state. Described here is an investigation of the compound's solution properties by nuclear magnetic resonance spectroscopy, density functional calculations, and oxygen isotope effects. The study yields two major findings. First, [Cu(η^1-O_2)TMG_3tren]$^+$ is paramagnetic due to a triplet electronic structure; this is in contrast to other copper compounds where O_2 is bound in a side-on manner. Second, the oxygen equilibrium isotope effect upon O_2 binding to copper(I) (^{18}O EIE $\equiv$ $K(^{16}O^{16}O)/K(^{16}O^{18}O)$ = 1.0148 ± 0.0012) is significantly larger than those determined for iron and cobalt η^1-O_2 adducts. This result is suggested to reflect greater ionic ($Cu^{II}-O_2^{-I}$) character within the valence bond description. A revised interpretation of the physical origins of the ^{18}O EIEs upon O_2 binding to redox metals is also advanced along with experimental data that should be used as benchmarks for interpreting ^{18}O kinetic isotope effects upon enzyme reactions.

1. Introduction

The coordination of molecular oxygen to a reduced iron or copper site is a primary step in aerobic respiration,[1] sensing of cellular redox status,[2] and catalysis by a wide variety of enzymes.[3−5] Mononuclear copper−dioxygen (CuO_2) intermediates have only fairly recently been characterized, and much remains to be understood regarding their reactivity.[6−9] For instance, in enzymes CuO_2 species have been proposed to oxidize C−H bonds.[4,5] Protein crystallography has provided support for such intermediates, although assessing their involvement during catalysis has remained a challenge.[8,9]

Our efforts have been concentrated on developing isotope fractionation techniques to probe oxidation reactions of metalloenzymes and inorganic compounds.[10−12] Presented here are findings which demonstrate the ability to predict and identify structures relevant to metal-mediated O_2 activation. Preliminary

[†] Johns Hopkins University.
[‡] University of Minnesota.
[§] Philipps-Universität Marburg.

(1) (a) Pauling, L.; Coryell, C. D. *Proc. Natl. Acad. Sci. U.S.A.* **1936**, *22*, 210−216. (b) Babcock, G. T.; Wikstrom, M. *Nature* **1992**, *356*, 301−309. (c) Takahashi, T.; Kuroiwa, S.; Ogura, T.; Yoshikawa, S. *J. Am. Chem. Soc.* **2005**, *127*, 9970−9971.
(2) (a) Haddad, J. J. *Biochem. Biophys. Res. Commun.* **2004**, *316*, 969−977. (b) Dioum, E. M.; Rutter, J.; Tuckerman, J. R.; Gonzalez, G.; Gilles-Gonzalez, M-A.; McKnight, S. L. *Science* **2002**, *298*, 2385−2387. (c) Ohta, T.; Yoshimura, H.; Yoshioka, S.; Aono, S.; Kitagawa, T. *J. Am. Chem. Soc.* **2004**, *126*, 15000−15001.
(3) (a) Valentine, J. S., Foote, C. S., Greenberg, A., Liebman, J. F., Eds. *Active Oxygen in Biochemistry*; Chapman & Hall: New York, 1995. (b) Holm, R. H.; Kennepohl, P.; Solomon, E. I. *Chem. Rev.* **1996**, *96*, 2239−2314. (c) Decker, A.; Solomon, E. I. *Curr. Opin. Chem. Biol.* **2005**, *9*, 152−163. (d) Bollinger, J. M.; Krebs, C. *Curr. Opin. Chem. Biol.* **2007**, *11*, 151−158.
(4) (a) Klinman, J. P. *J. Biol. Chem.* **2006**, *281*, 3013−3016. (b) Evans, J. P.; Ahn, K.; Klinman, J. P. *J. Biol. Chem.* **2003**, *278*, 49691−49698. (c) Francisco, W. A.; Blackburn, N. J.; Klinman, J. P. *Biochemistry* **2003**, *42*, 1813−1819.
(5) (a) Chen, P.; Solomon, E. I. *J. Am. Chem. Soc.* **2004**, *126*, 4991−5000. (b) Chen, P.; Bell, J.; Eipper, B. A.; Solomon, E. I. *Biochemistry* **2004**, *43*, 5735−5747.
(6) For reviews on synthetic mononuclear CuO_2 complexes see: (a) Cramer, C. J.; Tolman, W. B. *Acc. Chem. Res.* **2007**, *40*, 601−608. (b) Itoh, S. *Curr. Opin. Chem. Biol.* **2006**, *10*, 115−122. (c) Karlin, K. D.; Kaderli, S.; Zueberbuehler, A. D. *Acc. Chem. Res.* **1997**, *30*, 139−147.
(7) (a) Fujisawa, K.; Tanaka, M.; Moro-oka, Y.; Kitajima, N. *J. Am. Chem. Soc.* **1994**, *116*, 12079−10280. (b) Aboelella, N. W.; Lewis, E. A.; Reynolds, A. M.; Brennessel, W. W.; Cramer, C. J.; Tolman, W. B. *J. Am. Chem. Soc.* **2002**, *124*, 10660−10661. (c) Jazdzewski, B. A.; Reynolds, A. M.; Holland, P. L.; Young, V. G.; Kaderli, S.; Zuberbuehler, A. D.; Tolman, W. B. *J. Biol. Inorg. Chem.* **2003**, *8*, 381−393. (d) Weitzer, M.; Schindler, S.; Brehm, G.; Schneider, S.; Hoermann, E.; Jung, B.; Kaderli, S.; Zuberbuehler, A. D. *Inorg. Chem.* **2003**, *42*, 1800−1806. (e) Komiyama, K.; Furutachi, H.; Nagatomo, S.; Hashimoto, A.; Hayashi, H.; Fujinami, S.; Suzuki, M.; Kitagawa, T. *Bull. Chem. Soc. Jpn.* **2004**, *77*, 59−72. (f) Reynolds, A. M.; Gherman, B. F.; Cramer, C. J.; Tolman, W. B. *Inorg. Chem.* **2005**, *44*, 6989−6997. (g) Sarangi, R.; Aboelella, N.; Fujisawa, K.; Tolman, W. B.; Hedman, B.; Hodgson, K. O.; Solomon, E. I. *J. Am. Chem. Soc.* **2006**, *128*, 8286−8296. (h) Maiti, D.; Fry, H. C.; Woertink, J. S.; Vance, M. A.; Solomon, E. I.; Karlin, K. D. *J. Am. Chem. Soc.* **2006**, *129*, 264−265.
(8) Prigge, S. T.; Eipper, B. A.; Mains, R. E.; Amzel, L. M. *Science* **2004**, *304*, 836−837.
(9) Wilmot, C. M.; Hajdu, J.; McPherson, M. J.; Knowles, P. F.; Phillips, S. E. V. *Science* **1999**, *286*, 1724−1728.
(10) Smirnov, V. V.; Brinkley, D. W.; Lanci, M. P.; Karlin, K. D.; Roth, J. P. *J. Mol. Catal. A: Chem.* **2006**, *251*, 100−107.
(11) Roth, J. P.; Klinman, J. P. In *Isotope Effects in Chemistry and Biology*; Kohen, A., Limbach, H. H., Eds.; CRC Press: Boca Raton, 2005.
(12) Roth, J. P. *Curr. Opin. Chem. Biol.* **2007**, *11*, 142−150.

studies have suggested that oxygen equilibrium isotope effects (^{18}O EIEs) can be used to differentiate end-on (η^1) superoxide (O_2^{-I}) and side-on (η^2) peroxide (O_2^{-II}) species;[13,14] however, the theoretical basis for these observations had not been established.[10,13]

The isotope fractionation technique is extended to the characterization of CuO_2 species, which are currently the focus of synthetic modeling efforts.[6,7,15,16] The relationship of experimentally determined to computationally determined isotope effects is described. Analysis within the context of the accepted quantum mechanical theory sheds new light on the physical origins of the ^{18}O EIEs. The results can be used to interpret the oxygen kinetic isotope effects (^{18}O KIEs) which have now been measured for a number of copper-containing enzymes.[11,12]

We have examined the only synthetic copper compound shown by X-ray crystallography to contain molecular oxygen bound in an end-on fashion.[15,16] The solid-state structure of [Cu(η^1-O_2)TMG$_3$tren](SbF$_6$) (TMG$_3$tren = 1,1,1-tris{2-[*N*^{2}-(1,1,3,3-tetramethylguanidino)]ethyl}amine) was recently determined using cryogenic methods.[15] These experiments were quite challenging as the compound readily loses O_2 in the solid state at temperatures above 210 K. Through solution studies of the reversible O_2 binding equilibrium (eq 1) by nuclear magnetic resonance (NMR) spectroscopy, we have discovered that [Cu(η^1-O_2)TMG$_3$tren]$^+$ is paramagnetic. Magnetic susceptibility measurements on analytically pure samples at low temperatures in *N*,*N*-dimethylformamide (DMF) indicate the presence of two unpaired electrons. This observation is consistent with a triplet ground state, although it is presently unclear where exactly the electrons are localized. This unusual electronic structure for a metal−oxygen adduct, although proposed on the basis of computational studies,[17−20] has not, to our knowledge, been conclusively demonstrated by experiment.[21] The triplet state is most readily attributed to ferromagnetic coupling of an unpaired electron associated with copper(II) and an unpaired electron of the same spin associated with the superoxide ligand. Another possibility, although less commonly accepted, is copper(I) bound to oxygen containing two unpaired electrons of the same spin.

(1)

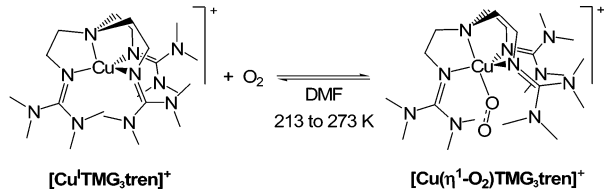

The oxygen isotope effect upon the equilibrium in eq 1 (^{18}O EIE = $K^{16,16}O_2/K^{16,18}O_2$) is determined by the change in vibrational frequencies of the reactant relative to the product. We describe here how the experimental value determined for [Cu(η^1-O_2)TMG$_3$tren]$^+$ can be reproduced remarkably well using density functional calculations. The agreement between theory and experiment validates our basic approach of using isotope effects together with computational methods to identify activated oxygen intermediates during enzyme catalysis.

Calculations are performed for other synthetic mononuclear CuO_2 compounds where the irreversible nature of O_2 binding has precluded ^{18}O EIE measurements. On the basis of the predicted values, end-on CuO_2 structures should be easily distinguished from the side-on structures. The analysis of isotope-dependent partition functions reveals the underlying enthalpic and entropic causes of the different ^{18}O EIEs. The emerging model provides a framework for future studies of heavy-atom isotope effects on transition metal-mediated activation of various small molecules.[11,12,22,23]

2. Experimental Section

2.1. General. Specialty chemicals were obtained from Sigma-Aldrich unless noted otherwise. Compressed gases were obtained from Airgas in the highest purity available. "Anhydrous" brand DMF was obtained from Burdick and Jackson and sparged with N_2 prior to use. Other solvents were obtained from EMD Chemicals and purified following standard protocols.[24] Deuterium-labeled compounds (tetramethylurea-d_{12}) and NMR solvents were obtained from Cambridge Isotope Laboratories.

Copper compounds were synthesized as the triflate (OTf = trifluoromethanesulfonate) salts according to the modified literature procedures presented below and in the Supporting Information.[25] Purity of the compounds was assessed by elemental analysis (Desert Analytics, Tucson, AZ), spectrophotometric determination of molar extinction coefficients, and NMR spectroscopy. Samples for ^{18}O EIE measurements were prepared using a home-built vacuum apparatus that allowed concurrent pressure measurements (manometry) on the O_2 binding reactions. The apparatus and procedures used to determine competitive

(13) (a) Lanci, M. P.; Roth, J. P. *J. Am. Chem Soc.* **2006**, *128*, 16006−16007. (b) Lanci, M. P.; Brinkley, D. W.; Stone, K. L.; Smirnov, V. V.; Roth, J. P. *Angew. Chem., Int. Ed.* **2005**, *44*, 7273−7276.
(14) The first indication that ^{18}O EIEs could serve as probes of activated oxygen structures derived from O_2 was published several years earlier: Tian, G.; Klinman, J. P. *J. Am. Chem. Soc.* **1993**, *115*, 8891−8897.
(15) Wurtele, C; Gaoutchenova, E.; Harms, K.; Holthausen, M. C.; Sundermeyer, J.; Schindler, S. *Angew. Chem., Int. Ed.* **2006**, *45*, 3867−3869.
(16) Schatz, M.; Raab, V.; Foxon, S. P.; Brehm, G.; Schneider, S.; Reiher, M.; Holthausen, M. C.; Sundermeyer, J.; Schindler, S *Angew. Chem., Int. Ed.* **2004**, *43*, 4360−4363.
(17) Most relevant to the present work are density functional calculations which have predicted a ground-state triplet structure for a copper−oxygen adduct isoelectronic and isostructural to that described in the present study. (a) de la Lande, A.; Moliner, V.; Parisel, O. *J. Chem. Phys.* **2007**, *126*, 035102/1−035102/7. (b) de la Lande, A.; Gerard, H.; Moliner, V.; Izzet, G.; Reinaud, O.; Parisel, O. *J. Biol. Inorg. Chem.* **2006**, *11*, 593−608.
(18) An early *ab initio* study predicted a ground-state triplet for the product formed upon reacting nickel(0) bis(alkyl)isocynanides with O_2. Jørgensen, K. A.; Swanstrøm, P. *Acta Chem. Scand.* **1992**, *46*, 82−86.
(19) The electronic structure proposed in ref 18 was later re-evaluated using electron correlation methods and a ground-state singlet with low-lying triplet states were found, consistent with the available experimental data. (a) Bytheway, I.; Hall, M. B. *Inorg. Chem.* **1995**, *34*, 3741−3746. (b) Bytheway, I.; Hall, M. B. *Chem. Rev.* **1994**, *94*, 639−658.
(20) Palladium(I) η^1-superoxide complexes, isoelectronic to the copper and nickel dioxygen compounds in refs 17−19 and 21, have been proposed as intermediates in the oxygenation of palladium(0) ligand complexes. On the basis of density functional calculations these species are proposed to have ground-state triplet structures. (a) Landis, C. R.; Morales, C. M.; Stahl, S. S. *J. Am. Chem. Soc.* **2004**, *126*, 16302−16303. (b) Popp, B. V.; Wendlandt, J. G.; Landis, C. R.; Stahl, S. S. *Angew. Chem., Int. Ed.* **2007**, *46*, 601−604.
(21) Chen, P.; Root, D. E.; Campochiaro, C.; Fujisawa, K.; Solomon, E. I. *J. Am. Chem. Soc.* **2003**, *125*, 466−474. This reference describes the possibility of a low-lying triplet excited state present in a solid-state sample of a side-on bound CuO_2 complex.
(22) Examples include isotopic studies of nitrogen fixation and O_2 evolution by photsystem II: (a) Sra, Amandeep, K.; Hu, Y.; Martin, G. E.; Snow, D. D.; Ribbe, M. W.; Kohen, A. *J. Am. Chem. Soc.* **2004**, *126*, 12768−12769. (b) Metzner, H.; Fischer, K.; Bazlen, O. *Biochim. Biophys. Acta* **1979**, *548*, 287−295. (c) Guy, R. D.; Fogel, M. L.; Berry, J. A. *Plant Phys.* **1993**, *101*, 37−47. (d) Burda, K.; Bader, K. P.; Schmid, G. H. *Biochim. Biophys. Acta: Bioenerg.* **2003**, *1557*, 77−82.
(23) (a) Purdy, M. M.; Koo, L. S.; Ortiz de Montellano, P. R.; Klinman, J. P. *Biochemistry* **2006**, *45*, 15793−15806. (b) Mure, M.; Mills, S. A.; Klinman, J. P. *Biochemistry* **2002**, *41*, 9269−9278. (c) Stahl, S. S.; Francisco, W. A.; Merkx, M.; Klinman, J. P.; Lippard, S. J. *J. Biol. Chem.* **2001**, *276*, 4549−4553. (d) Francisco, W. A.; Tian, G.; Fitzpatrick, P. F.; Klinman, J. P. *J. Am. Chem. Soc.* **1998**, *120*, 4057−4062. (e) Tian, G.; Berry, J. A.; Klinman, J. P. *Biochemistry* **1994**, *33*, 226−234.
(24) See the Supporting Information.
(25) Raab, V.; Kipke, J.; Burghaus, O.; Sundermeyer, J. *Inorg. Chem.* **2001**, *40*, 6964−6971.

oxygen isotope effects on reactions of natural abundance O_2 have been described elsewhere.[10]

NMR spectra were recorded using Varian Unity Inova 500 MHz and Bruker Avance 300 MHz spectrometers. The temperature inside the spectrometer was checked using Van Geet's method.[26] NMR samples were prepared in tubes equipped with resealable Teflon valves (J. Young). Solutions were saturated with the appropriate gas mixture at the experimental temperature and ambient pressure. Magnetic susceptibility measurements were performed following Evans' method[27] as detailed below. Chemical shifts are quoted in ppm versus the residual solvent signals, and integrated peak areas are relative to an internal standard of known concentration; hexamethyldisiloxane (HMDS) was typically used for this purpose. Electron paramagnetic resonance (EPR) spectra were recorded on X-band Bruker EMX and ESP 300E spectrometers at temperatures between 4 and 230 K.

2.2. Synthesis and Characterization of Compounds. 2.2.1. [Cu^{I}TMG$_3$tren](OTf). [Cu^{I}TMG$_3$tren]$^{1+}$ was prepared by reacting bis-[triflate copper(I)]·benzene (90%) (231 mg, 458 mmols) with TMG$_3$-tren (430 mg, 989 mmols) in anhydrous, deoxygenated acetonitrile. The copper(I) triflate solution (8 mL) was added dropwise to the ligand solution (8 mL) at room temperature. The reaction mixture, after stirring for 45 min, appeared pale yellow. This solution was filtered through Celite and concentrated to 4 mL. The filtrate was layered with 30 mL of diethyl ether. Slow diffusion of the ether layer afforded colorless crystals in 79% yield. ^{1}H NMR (300 MHz, DMF-d_7, 298 K) $\delta = 3.26$ (vt, 6 H, CH_2), 2.78 (s, 18 H, CH_3), 2.71 (s, 18 H, CH_3), 2.64 (vt, 6 H, CH_2); ^{13}C{^{1}H} NMR (75.5 MHz, DMF-d_7, 298 K) $\delta = 160.0$ (CN_3), 50.7 (CH_2), 47.1 (CH_2), 37.5 (CH_3), 37.4 (CH_3). Elemental analysis: *calcd* for $C_{22}H_{48}N_{10}O_3F_3SCu$: 40.45 C, 7.41 H, 21.44 N; *found:* 40.58 C, 7.07 H, 21.35 N.

[Cu^{I}TMG$_3$tren](OTf)-d_{36} was prepared from TMG$_3$tren-d_{36} as described above. The isolated yield based upon copper was 81%; ^{1}H NMR (500 MHz, DMF-d_7, 298 K) $\delta = 3.26$ (vt, 6 H, CH_2), 2.63 (vt, 6 H, CH_2); ^{2}H NMR (76.8 MHz, DMF, 298 K) $\delta = 2.73$ (s, 18 H, CH_3), 2.65 (s, 18 H, CH_3); ^{13}C{^{1}H} NMR (75.5 MHz, DMF-d_7, 298 K) $\delta = 160.1$ (CN_3), 120.2 (quartet, $^1J_{C-F} = 322.7$ Hz, S−C−F_3), 50.8 (s, CH_2), 47.0 (s, CH_2), 37.5 (septet, $^1J_{C-D} = 20.8$ Hz, CD_3), 37.4 (septet, $^1J_{C-D} = 20.7$ Hz, CD_3). Elemental analysis: *calcd* for $C_{22}H_{12}D_{36}N_{10}O_3F_3SCu$: 38.32 C, 7.02 D, 20.31 N; *found:* 38.04 C, 6.78 D, 20.31 N. This analytical method does not distinguish deuterium from protium.

2.2.2. [Cu^{II}TMG$_3$tren](OTf)$_2$. [Cu^{II}TMG$_3$tren]$^{2+}$ was prepared using Cu^{II}(OTf)$_2$ and the procedure outlined for [Cu^{I}TMG$_3$tren](OTf). Emerald green crystals were obtained in 80% yield. Elemental analysis: *calcd* for $C_{25}H_{51}N_{10}O_6F_6S_2Cu$: 35.60 C, 6.09 H, 18.27 N; *found:* 35.97 C, 6.18 H, 18.24 N. The following extinction coefficients were determined in DMF at 298 K: $\epsilon_{388\ nm} = 960 \pm 170$ M^{-1} cm^{-1} (shoulder), $\epsilon_{773\ nm} = 73 \pm 15$ M^{-1} cm^{-1} and $\epsilon_{1056\ nm} = 300 \pm 53$ M^{-1} cm^{-1}.

2.2.3. [Cu(η^1-O$_2$)TMG$_3$tren](OTf). [Cu(η^1-O$_2$)TMG$_3$tren]$^+$ was generated *in situ* by reacting a solution of analytically pure [Cu^{I}TMG$_3$-tren]$^{1+}$ with O_2 at low temperature. In a typical experiment, a weighed amount of the copper(I) compound was dissolved in the appropriate solvent under N_2 and cooled to the experimental temperature. An NMR spectrum was obtained, and the diamagnetic signals were quantified versus an internal standard. Exposure to O_2 caused the solution to turn from colorless to green. Analysis of the NMR spectrum at this point revealed paramagnetically shifted and broadened signals with the following integral areas: ^{1}H NMR (300 MHz, DMF-d_7, 213 K) $\delta =$ 301 (br s, 3 H, H−CH), 67.1 (br s, 3 H, H−CH), 21.9 (br s, 9 H, CH_3), 16.2 (br s, 9 H, CH_3), 15.2 (br s, 9 H, CH_3), 7.2 (br s, 3 H, H−CH), 6.2 (br s, 9 H, CH_3), and −5.5 (br s, 3 H, H−CH).

Spectral assignments were confirmed by analysis of [Cu(η^1-O$_2$)TMG$_3$tren]$^+$-d_{36} in which the methyl groups were labeled with deuterium. ^{1}H NMR (500 MHz, DMF-d_7, 213 K) $\delta = 294.9$ (br s, 3 H, H−CH), 65.3 (br s, 3 H, H−CH), 7.2 (br s, 3 H, H−CH), and −5.2 (br s, 3 H, H−CH); ^{2}H NMR (76.8 MHz, DMF, 213 K) $\delta = 20.8$ (br s, 9 H, CH_3), 16.2 (br s, 9 H, CH_3), 14.4 (br s, 9 H, CH_3), and 6.2 (br s, 9 H, CH_3). The ^{2}H resonances in [Cu(η^1-O$_2$)TMG$_3$tren]$^+$-d_{36} are sharpened by approximately a factor of 7 relative to the ^{1}H resonances of [Cu(η^1-O$_2$)TMG$_3$tren]$^+$ at the same field. This sharpening is due to the decreased gyromagnetic constant associated with deuterium.

2.3. Solution Magnetic Susceptibility Measurements.[24,27] A standard solution containing a known concentration of internal standard (HMDS) was prepared in DMF-d_7 inside a N_2-filled glove box. This solution was partitioned and a portion used to dissolve a weighed amount of [Cu^{I}TMG$_3$tren](OTf). Solutions with and without copper were placed in separate vials, sealed with rubber septa under N_2, and chilled to the experimental temperature. The solutions were then oxygenated by rapid stirring under air or O_2 for at least 1 h.

The standard solution without copper was transferred by cannula into a prechilled NMR tube. The coaxial insert (New Era Enterprises) was subsequently placed inside this tube under the appropriate atmosphere. The equilibrated [Cu(η^1-O$_2$)TMG$_3$tren]$^+$ solution was then transferred into the coaxial insert and the tube sealed at 1 atm. Care was taken to ensure that the samples remained at constant temperature (213 K or 247 K) during all manipulations to avoid changes in the concentration of O_2.

The magnetic susceptibility, χ_g (mL/g), was calculated from the frequency shift of HMDS ($\Delta\nu$ in Hz) and the concentration of [Cu(η^1-O$_2$)TMG$_3$tren]$^+$ (m in g/mL) according to eq 2.[28] Control experiments with *tert*-butanol and 1,4-dioxane as the internal standards confirmed the nonspecific nature of the paramagnetic shift.[29] The concentration of [Cu(η^1-O$_2$)TMG$_3$tren]$^+$ was calculated on the basis of the concentration of O_2 at the experimental temperature[30] and the equilibrium constant for O_2 binding to [Cu^{I}TMG$_3$tren]$^+$ (K_{O2}). The K_{O2} was determined independently by manometry as described below. The temperature dependence of the DMF-d_7 density was taken into consideration through the empirically derived expression: d(g/mL) = 1.344 − 0.001012 × T(K).

$$\chi_g = \left(-\frac{3}{4\pi}\right)\left(\frac{\Delta\nu}{\nu}\right)\left(\frac{1}{m}\right) \qquad (2)$$

The molar magnetic susceptibility, χ_m (mL/mol), was calculated from χ_g and the molecular weight of [Cu(η^1-O$_2$)TMG$_3$tren]$^+$ (536.24 g/mol). Corrections for the diamagnetic contribution, χ_m^d, associated with [Cu(η^1-O$_2$)TMG$_3$tren]$^+$, [Cu^{I}TMG$_3$tren]$^+$, and the triflate counterions, were applied in order to obtain the molar paramagnetic susceptibility, χ_m^p.[31] The χ_m^p values were then used to estimate the effective magnetic moment, μ_{eff}, in units of the Bohr magneton (β), according to eq 3; the calculation includes the temperature (T), Boltzmann's constant (k), and Avogadro's number (N_A).

$$\mu_{eff} = \sqrt{\frac{3kT\chi_m^p}{N_A\beta}} \qquad (3)$$

2.4. Procedure for Measuring Equilibrium Isotope Effects. The oxygen equilibrium isotope effect is defined as the ratio of equilibrium constants for the binding of $^{16,16}O_2$ and $^{16,18}O_2$ to [Cu^{I}TMG$_3$tren]$^+$ according to eq 1, i.e., $K(^{16}O^{16}O)/K(^{16}O^{18}O)$. This ratio was determined by analyzing the isotope composition of the O_2 released from [Cu(η^1-O$_2$)TMG$_3$tren]$^+$ using an isotope ratio mass spectrometry method. The detailed procedure has been published[10,11,13,14] and a brief description is provided below.

(26) Van Geet, A. L. *Anal. Chem.* **1970**, *42*, 679−680.
(27) Evans, D. F. *J. Chem. Soc.* **1959**, 2003−2005.
(28) Sur, S. K. *J. Magn. Reson.* **1989**, *82*, 169−173.
(29) Bertini, I.; Luchinat, C.; Turano, P.; Battaini, G.; Casella, L. *Chem. Eur. J.* **2003**, *9*, 2316−2322.
(30) The solubility of O_2 was determined at varying temperatures in DMF as described in ref 13a.
(31) O'Connor, C. J. *Progress in Inorganic Chemistry*; Lippard, S. J., Eds.; Wiley & Sons: New York, 1982; pp 203−213.

Samples of [Cu^{I}TMG$_3$tren]OTf (0.6−8.0 mM) were pre-equilibrated in air-saturated DMF solutions at low temperatures. The O_2 was isolated before and after adding the copper(I) compound. Thus, the ^{18}O:^{16}O content of the O_2 derived from [Cu(η^1-O_2)TMG$_3$tren]$^+$ could be determined relative to the ^{18}O:^{16}O present in air at natural abundance levels. The solutions containing copper reached equilibrium rapidly, yet they were typically maintained at the experimental temperature for 1−5 h prior to collection of the O_2. Quantitative isolation of O_2 was achieved by sparging a fixed volume of solution with helium under dynamic vacuum. The O_2 in the helium carrier gas was passed through a series of traps cooled with liquid nitrogen to remove volatile solvent, water vapor, and CO_2. The O_2 was collected on 5 Å molecular sieves, and the helium was removed by evacuation. The O_2 was then quantitatively converted to CO_2 by combustion at 900 °C over graphite with a platinum catalyst. The pressure of the CO_2 was determined using a capacitance manometer, and then the gas was flame sealed in a dry glass sample tube for later isotope ratio mass spectrometry (IRMS) analysis. Isotope effects were calculated according to eq 4. The IRMS afforded ^{18}O:^{16}O versus a standard (e.g., standard mean ocean water, SMOW) with a typical error of ±0.0002 (0.2 ppm).

The precision of the measurements owes to the fact that the ^{18}O EIE comes from a ratio of ratios. In eq 4, R_t is the ^{18}O:^{16}O in the "total" O_2 isolated from the [Cu(η^1-O_2)TMG$_3$tren]$^+$-containing solutions. R_u is the ^{18}O:^{16}O of the "unbound" O_2 isolated from solutions that do not contain copper. The $1 - f$ is the fraction of the total O_2 which is bound to copper at equilibrium. Measurements were performed using solutions freshly prepared from different lots of solvent and [Cu^{I}TMG$_3$tren](OTf). The ^{18}O EIE at each temperature was determined from multiple independent measurements and reported with an error reflecting one standard deviation about the mean.

$$^{18}\text{O EIE} = \frac{K(^{16}O^{16}O)}{K(^{16}O^{18}O)} = \frac{1-f}{R_t/R_u - f} \tag{4}$$

2.5. Calculation of Equilibrium Isotope Effects. For the end-on binding of O_2 to copper(I) in eq 1 where $K(O_2) = [CuO_2]/[Cu^I][O_2]$ the ^{18}O EIE is defined according to eq 4. Under the experimental conditions, the $^{16,16}O_2$ and $^{16,18}O_2$ isotopologues of O_2 react competitively with copper(I). Thus, the ^{18}O EIE is determined from the equilibrium concentrations of "bound" and "unbound" O_2 according to:

$$^{18}\text{O EIE} = \frac{[Cu^{16,16}O_2]}{[^{16,16}O_2]} \Big/ \frac{[Cu^{16,18}O_2]}{[^{16,18}O_2]} = \frac{[Cu^{16,16}O_2][^{16,18}O_2]}{[Cu^{16,18}O_2][^{16,16}O_2]} \tag{5}$$

The right part of eq 5 expresses the equilibrium constant for an isotope exchange reaction, such as that shown in eq 6a. When a side-on CuO_2 product is formed and the oxygen nuclei are equivalent by symmetry, only one isotope exchange reaction is required.

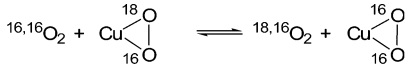

(6a)

When an end-on CuO_2 product is formed, it is necessary to consider two isotope exchange reactions, as shown in eqs 6b and 6c.[32] The initial and final states of the O_2 are designated A and B, respectively, with the asterisk marking the site of the heavy isotope. The two equilibria differ with respect to the identity of B*, i.e. whether O_2 is bound to copper through ^{16}O or ^{18}O. Throughout this study, the simplifying assumption is made that B* consists of a 50/50 mixture of Cu−$^{16}O^{18}O$ and Cu−$^{18}O^{16}O$. Neglecting a small (ca. 1%) isotope effect due to the preferred coordination of ^{16}O to the copper causes the calculated ^{18}O EIE to be slightly underestimated, the variation occurring in the fourth decimal place.

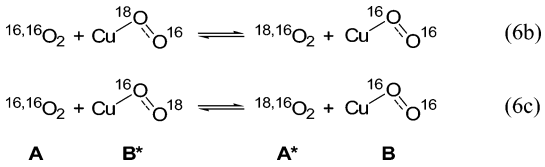

The approach of Bigeleisen and Goeppert-Mayer[32] was used to calculate the ^{18}O EIEs from the partition functions associated with the $^{16}O^{16}O$ and $^{16}O^{18}O$ isotopologues (eq 7). These isotope-dependent partition functions corresponding to zero-point energy (ZPE), vibrational excited-state energy (EXC), and the mass and moments of inertia (MMI) can be expressed in terms of stretching frequencies (eqs 8−10). The definition of MMI as a vibrational product (VP) derives from the Redlich−Teller product rule; the application of which requires using all of the vibrational modes.[33] MMI can also be calculated according to a classical expression (eq 11) which is based only on the masses (M) and the rotational moments of inertia (I). The latter values as well as the stretching frequencies were determined from density functional calculations on fully optimized geometries.

$$^{18}\text{O EIE}_{calc} = \text{MMI} \times \text{EXC} \times \text{ZPE} \tag{7}$$

$$\text{ZPE} = \frac{\left[\prod_j^{3N-6} \frac{\exp^{(h\nu_j^{B*}/2kT)}}{\exp^{(h\nu_j^{B}/2kT)}}\right]}{\left[\prod_i^{3N-5} \frac{\exp^{(h\nu_i^{A*}/2kT)}}{\exp^{(h\nu_i^{A}/2kT)}}\right]} \tag{8}$$

$$\text{EXC} = \frac{\left[\prod_j^{3N-6} \frac{1-\exp^{-(h\nu_j^{B*}/kT)}}{1-\exp^{-(h\nu_j^{B}/kT)}}\right]}{\left[\prod_i^{3N-5} \frac{1-\exp^{-(h\nu_i^{A*}/kT)}}{1-\exp^{-(h\nu_i^{A}/kT)}}\right]} \tag{9}$$

$$\text{MMI} = \text{VP} = \frac{\prod_j^{3N-6} (\nu_j^{B}/\nu_j^{B*})}{\prod_i^{3N-5} (\nu_i^{A}/\nu_i^{A*})} \tag{10}$$

$$\text{MMI} = \frac{\left[\left(\frac{M_{16-16}}{M_{16-18}}\right)^{3/2} \prod_i^{n_{rot}} \left(\frac{I_{i,16-16}}{I_{i,16-18}}\right)^{1/2}\right]_{final}}{\left[\left(\frac{M_{16-16}}{M_{16-18}}\right)^{3/2} \prod_i^{n_{rot}} \left(\frac{I_{i,16-16}}{I_{i,16-18}}\right)^{1/2}\right]_{initial}} \tag{11}$$

2.6. Density Functional Calculations. Molecular geometries were fully optimized at the density functional level of theory (DFT) using the exchange and correlation functionals of Perdew and co-workers[34] as modified by Adamo and Barone (*m*PWPW91).[35] Atomic orbital basis functions were taken for Cu from the compact relativistic effective core potential basis CEP-31G,[36] for N and O from the 6-311G* basis, for C from the 6-31G basis, and for H from the minimal STO-3G basis.[37]

(32) Bigeleisen, J.; Goeppert-Mayer, M. *J. Chem. Phys.* **1947**, *15*, 261−267.
(33) Wilson, E. B., Jr.; Decius, J. C.; Cross, P. C. *Molecular Vibrations*; Dover: New York, 1980; pp 182−193.
(34) (a) Perdew, J. P.; Wang, Y. *Phys. Rev. B* **1986**, *33*, 8800−8802. (b) Perdew, J. P. In *Electronic Structure of Solids '91*; Ziesche, P., Eschrig, H., Eds.; Akademie Verlag: Berlin, 1991; pp 11−20.
(35) Adamo, C.; Barone, V. *J. Chem. Phys.* **1998**, *108*, 664−675.

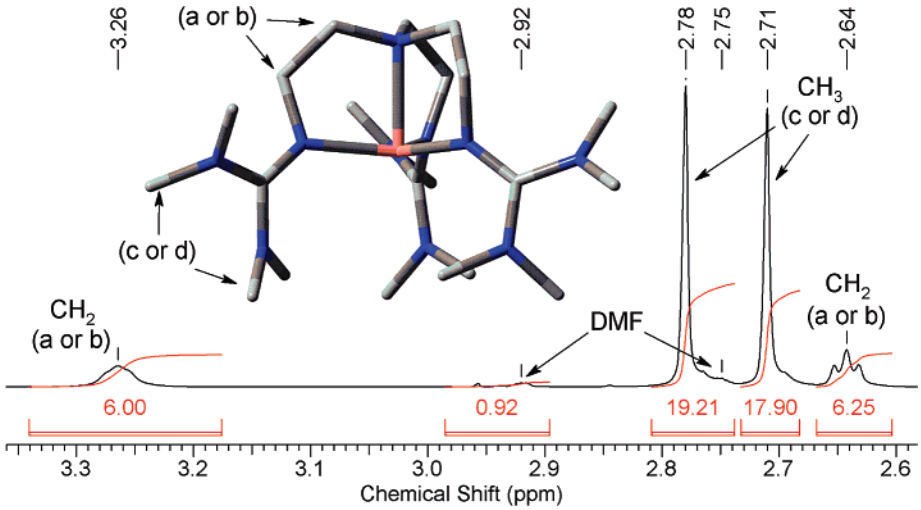

Figure 1. ^{1}H NMR spectrum (500 Mhz) of $[Cu^I(TMG_3tren)]^{1+}$ in DMF-d_7 at 298 K.

Unrestricted Kohn−Sham (KS) DFT was used for the triplet states as well as for the broken-symmetry (BS) states that mix singlet and triplet character for equal numbers of α and β electrons (such states are sometimes called unrestricted singlets, but this is a misnomer since the spin state is usually far from pure).[38] In order to eliminate triplet spin contamination from the broken-symmetry KS self-consistent field (SCF) energies, purified singlet energies, were computed according to:[39]

$$E_{\text{singlet}} = \frac{2E_{\langle S_z\rangle=0} - \langle S^2\rangle E_{\langle S_z\rangle=1}}{2 - \langle S^2\rangle} \qquad (12)$$

The triplet energy is computed for the single-determinantal high-spin configuration $S_z = 1$ (at the BS geometry), and $\langle S^2\rangle$ is the expectation value of the total-spin operator applied to the KS determinant for the unrestricted BS $S_z = 0$ calculation.

For comparison purposes, restricted KS DFT was also carried out for singlet states; the restricted KS SCF solutions were unstable to spin-symmetry, breaking in every case. Vibrational frequencies were calculated analytically within the harmonic oscillator approximation.[38] All minima were characterized by real frequencies[24] unless noted otherwise.

Solvation effects were included in certain calculations using the polarized continuum model[40] (PCM) in its integral-equation formalism[41] (IEF-PCM). Default parameters for acetone as implemented in *Gaussian 03*[42] were chosen because the experimental resonance Raman data for $[Cu(\eta^1\text{-}O_2)TMG_3tren]^+$ have been reported in this solvent.[16]

3. Results

3.1. Characterization of Reversible O_2-Binding. $[Cu^ITMG_3tren]^+$ undergoes rapid and reversible oxygenation in solvents of varying polarity. The O_2 affinity increases in proportion to the solvent dielectric constant with $K_{O2} \sim 14$ times greater in DMF ($\epsilon = 36.7$) than in chlorobenzene ($\epsilon = 2.7$) at 247 K.[43] Similar behavior has been reported for cobalt(II) Schiff's base and porphyrin compounds which also form η^1-O_2 structures.[44,45] In the present study, NMR spectral changes reflecting the formation of the paramagnetic $[Cu(\eta^1\text{-}O_2)TMG_3tren]^+$ compound were correlated to O_2 uptake using manometry.

3.1.1. ^{1}H and ^{2}H NMR Studies. There are eight chemically inequivalent protons on each arm of the tripodal ligand in the static structure of $[Cu^I(TMG_3tren)]^+$, yet the ^{1}H NMR spectrum in DMF-d_7 at 293 K reveals only four resonances: two broad multiplets and two singlets integrating 6:6 and 18:18, respectively (Figure 1). The spectrum arises from rapid equilibration of the two sets of diastereotopic methylene protons and methyl groups on the NMR time scale. Consistent with this explanation, lowering the temperature results in broadening of the signals and eventual decoalescence. The diastereotopic methylene protons exhibit an a,a′,b,b′ pattern, and the methyl groups appear as a c,c′,d,d′ pattern at 213 K.[24] The $[Cu^I(TMG_3tren)]^+$-d_{36} compound with deuterium labeling at each methyl group behaves in the same manner, as indicated by analysis of the ^{1}H and ^{2}H NMR spectra.[24]

Exposure of the copper(I)-containing DMF-d_7 solution to O_2 at 273 K results in the disappearance of the characteristic ^{1}H NMR spectrum due to $[Cu^ITMG_3tren]^+$ and the appearance of broad signals in the diamagnetic region. Lowering the temperature shifts the equilibrium to favor $[Cu(\eta^1\text{-}O_2)TMG_3tren]^+$, revealing several signals between −6 and 300 ppm at 213 K (Figure 2). Assignments of these signals were made through comparisons to the compound with deuterium-labeled methyl groups on the ligand. The ^{1}H spectrum of $[Cu(\eta^1\text{-}O_2)TMG_3tren]^+$-$d_{36}$ consists of four diastereotopic methylene protons, and

(36) Stevens, W. J.; Krauss, M.; Basch, H.; Jasien, P. G. *Can. J. Chem.* **1992**, *70*, 612−629.
(37) Hehre, W. J.; Radom, L.; Schleyer, P. v. R.; Pople, J. A. *Ab Initio Molecular Orbital Theory*; Wiley: New York, 1986.
(38) Cramer, C. J. *Essentials of Computational Chemistry*, 2nd ed.; Wiley: Chichester, 2004.
(39) (a) Ziegler, T.; Rauk, A.; Baerends, E. J. *Theor. Chim. Acta* **1977**, *43*, 261−271. (b) Noodleman, L.; Norman, J. G. *J. Chem. Phys.* **1979**, *70*, 4903−4906. (c) Yamaguchi, K.; Jensen, F.; Dorigo, A.; Houk, K. N. *Chem. Phys. Lett.* **1988**, *149*, 537−542. (d) Lim, M. H.; Worthington, S. E.; Dulles, F. J.; Cramer, C. J. In *Chemical Applications of Density Functional Theory*; Laird, B. B., Ross, R. B., Ziegler, T., Eds.; American Chemical Society: Washington, DC, 1996; Vol. 629, pp 402−422. (e) Isobe, H.; Takano, Y.; Kitagawa, Y.; Kawakami, T.; Yamanaka, S.; Yamaguchi, K.; Houk, K. N. *Mol. Phys.* **2002**, *100*, 717−727.
(40) (a) Miertus, S.; Scrocco, E.; Tomasi, J. *Chem. Phys.* **1981**, *55*, 117−129. (b) Tomasi, J. In *Structure and Reactivity in Aqueous Solution*; Cramer, C. J., Truhlar, D. G., Eds.; American Chemical Society: Washington, DC, 1994; Vol. 568, pp 10−23.
(41) (a) Cancès, E.; Mennucci, B.; Tomasi, J. *J. Chem. Phys.* **1997**, *107*, 3032−3041. (b) Mennucci, B.; Tomasi, J. *J. Chem. Phys.* **1997**, *106*, 5151−5158. (c) Cossi, M.; Scalmani, G.; Rega, N.; Barone, V. *J. Chem. Phys.* **2002**, *117*, 43−54.
(42) Frisch, M. J.; et al. *Gaussian 03*; Gaussian, Inc.: Pittsburgh, PA, 2003.
(43) Lide, D. R. *CRC Handbook of Chemistry and Physics*, 74th ed.; CRC Press: Boca Raton, 1993. The dielectric constants of DMF and acetone are 38.9 and 21, respectively, at 298.15 K.
(44) Trovog, B. S.; Kitko, D. J.; Drago, R. S. *J. Am. Chem. Soc.* **1976**, *98*, 5144−5153.
(45) Walker, F. A. *J. Am. Chem. Soc.* **1973**, *95*, 1154−1159.

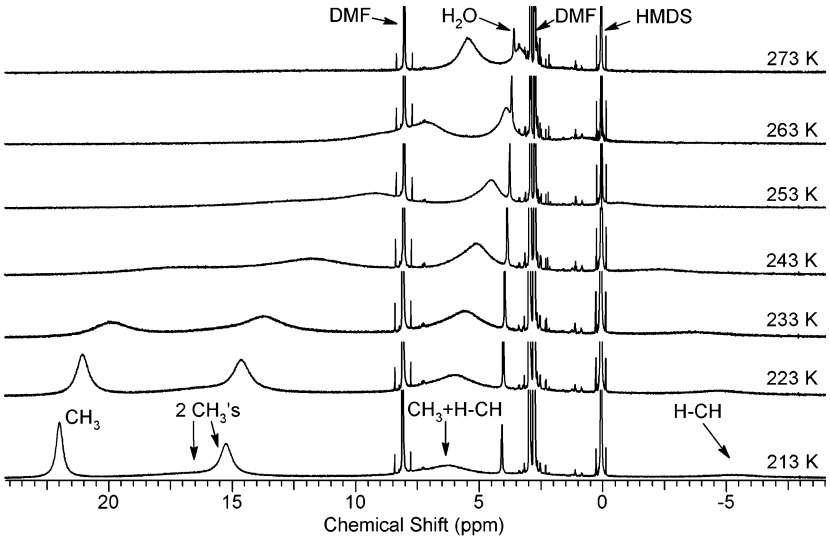

Figure 2. ^{1}H NMR spectra (300 Mhz) revealing the increased concentration of $[Cu(\eta^1\text{-}O_2)TMG_3tren]^+$ in O_2-saturated DMF-d_7 as the temperature is lowered from 273 to 213 K. The internal standard, hexamethyldisiloxane (HMDS) is noted. Only the region between 28 and −9 ppm is shown. Additional signals are observed at ∼65 and 300 ppm.

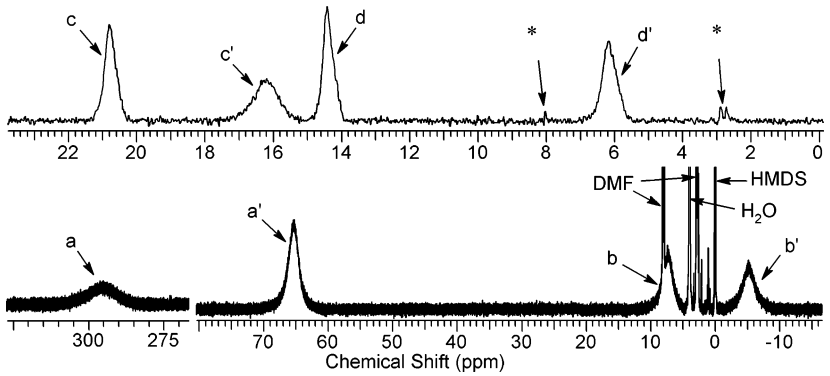

Figure 3. (Top) ^{2}H NMR spectrum (76.8 MHz) of $[Cu(\eta^1\text{-}O_2)TMG_3tren]^+$-$d_{36}$ in DMF at 213 K. (Bottom) ^{1}H NMR spectrum (500 MHz) of the same compound in DMF-d_7 at 213 K. Hexamethyldisiloxane (HMDS) is noted. The asterisks designate residual deuterium in DMF.

the ^{2}H spectrum consists of four diastereotopic methyl groups at 213 K (Figure 3). The latter signals are approximately 7 times sharper than those of the per-protio analogue (as expected, due to smaller gyromagnetic constant of ^{2}H relative to ^{1}H).

Importantly, the spectral changes associated with forming $[Cu(\eta^1\text{-}O_2)TMG_3tren]^+$ are completely reversed upon removing O_2 from the sample.[24] Integration of the NMR signals versus an internal standard reveals that $[Cu^{I}TMG_3tren]^+$ is recovered in 94 ± 6% yield. This observation indicates that a hypothetical Cu^{II}-containing decomposition product can be ruled out as the cause of the paramagnetically shifted and broadened NMR spectra (cf. Figures 2 and 3). The NMR results were corroborated by manometry under the analogous conditions. For instance, samples prepared at low O_2 concentration (0.2 mM) contained resolvable signals due to $[Cu(\eta^1\text{-}O_2)TMG_3tren]^+$ and $[Cu^{I}TMG_3tren]^+$.[24] The equilibrium constant determined by NMR integration, $K_{O2} = 3030 \pm 1200\ M^{-1}$ agreed reasonably well with the $K_{O2} = 4340 \pm 600\ M^{-1}$ determined from the O_2 pressure measurements.

The presence of a significant concentration of $[Cu^{II}TMG_3tren]^{2+}$, which could potentially form together with unbound superoxide ($O_2^{\bullet-}$) upon oxygenation of $[Cu^{I}TMG_3tren]^+$, can also be ruled out as the cause of the paramagnetic NMR spectrum. Evidence to this effect includes the observation that the peak positions as well as the line widths within the ^{1}H NMR spectra of $[Cu^{I}TMG_3tren]^+$ and $[Cu(\eta^1\text{-}O_2)TMG_3tren]^+$ are unchanged by the addition of $[Cu^{II}TMG_3tren]^{2+}$.[24] In addition, $[Cu(\eta^1\text{-}O_2)TMG_3tren]^+$ exhibits no discernible EPR signal at X-band frequency, under conditions where $[Cu^{II}TMG_3tren]^{2+}$ can be readily quantified.[24,46] While the absence of an EPR signal is a negative result, it is consistent with the proposed triplet state of $[Cu(\eta^1\text{-}O_2)TMG_3tren]^+$. Integer spin systems can be difficult to observe at X-band frequency due to the large zero-field splitting associated with dipole−dipole interaction of the unpaired electrons.[47]

3.1.2. Solution Magnetic Susceptibility. Measurements employing Evans' method[27,28] indicate that $[Cu(\eta^1\text{-}O_2)TMG_3tren]^+$ exhibits a magnetic moment that is relatively insensitive to temperature (Figure 4). Values of $\mu_{eff} = 3.21 \pm 0.26\ \mu_B$ (213 K) and $3.15 \pm 0.25\ \mu_B$ (247 K) were obtained by measuring the paramagnetic shift associated with the oxygenated copper compound. Analyses were performed in the presence of O_2 and the diamagnetic $[Cu^{I}TMG_3tren]^+$ as outlined in **Experimental Section 2.3**. The paramagnetic susceptibility of $[Cu(\eta^1\text{-}O_2)TMG_3tren]^+$ is only slightly smaller in the absence of the diamagnetic correction: $\mu_{eff,uncorr} = 3.12 \pm 0.27\ \mu_B$ at 213 K and 3.04 ±

(46) Gauchenova, E. V. Chemie superbasischer Chelatliganden für H^+, Cu^+ und Mn^{2+}. Ph.D. Thesis, Fachbereich Chemie, Philipps-Universität Marburg, Hans-Meerwein-Strasse, 35032 Marburg, Germany 2006.
(47) Drago, R. S. *Physical Methods for Chemists*, 2nd ed.; Surfside Scientific Publishers: Gainesville, 1992; pp 390−392.

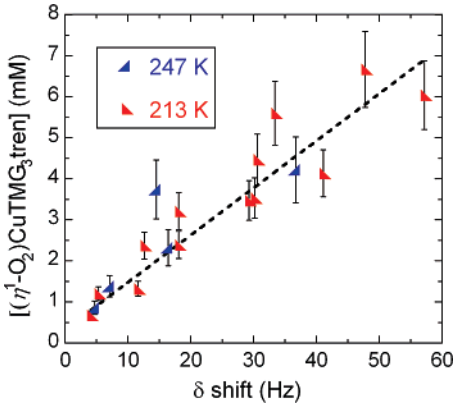

Figure 4. Determination of the solution magnetic moment of $[Cu(\eta^1\text{-}O_2)TMG_3tren]^+$. Data at 213 K and 247 are shown on one correlation line to illustrate the temperature insensitivity of μ_{eff}.

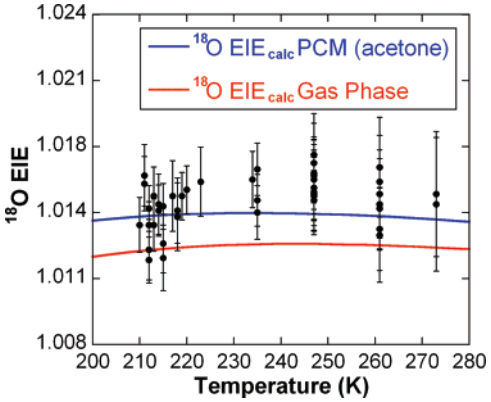

Figure 5. Oxygen equilibrium isotope effects (^{18}O EIEs) upon the formation of $[Cu(\eta^1\text{-}O_2)TMG_3tren]^+$ in DMF (eq 1). The red curve represents values calculated in the gas phase, and the blue curve represents values calculated using the polarized continuum model (PCM) and eqs 7−10.

0.26 μ_B at 247 K. The average magnetic moment is within error of the spin-only value of 2.83 μ_B calculated for a ground-state triplet species. A similar $\mu_{eff} = 3.02 \pm 0.25$ μ_B has been estimated in acetone at 190 K under the assumption that $[Cu(\eta^1\text{-}O_2)TMG_3tren]^+$ is formed quantitatively from $[Cu^ITMG_3tren]^+$ and O_2.[46]

3.1.3. Temperature Dependence of the Equilibrium Constant. Equilibrium constants corresponding to the formation of $[Cu(\eta^1\text{-}O_2)TMG_3tren]^+$ were determined by manometry.[24] K_{O2} at each temperature was extracted from several independently prepared samples. Pressure changes were related to the moles of O_2 taken up upon addition of a known concentration of $[Cu^ITMG_3tren]^+$ to air-saturated DMF. The O_2 obtained from the pre-equilibrated solutions varied in response to the concentration of $[Cu^ITMG_3tren]^+$ as expected for a 1:1 adduct. The manometry results could not be fitted to the equilibrium expression for a 2:1 adduct, consistent with $[Cu(\eta^1\text{-}O_2)TMG_3tren]^+$ as the only copper-oxygen adduct present in solution. This observation is also consistent with the NMR analysis described above.

The temperature dependence of K_{O2} was analyzed between 213 and 273 K. The $\Delta H = -8.4 \pm 0.8$ kcal mol^{-1} and $\Delta S = -23 \pm 3$ cal mol^{-1} K^{-1} (at 1 atm O_2) appear to be typical for formation of η^1-O_2 structures irrespective of the solvent polarity.[13a,48] The reaction exothermicity and competing unfavorable reaction entropy accounts for the common observation that end-on O_2 binding to copper(I) and cobalt(II) is rendered favorable by lowering the temperature.[44,45,48]

3.1.4. Equilibrium Isotope Effect upon O_2 Binding. ^{18}O EIEs were determined from the ^{18}O-enrichment of $[Cu(\eta^1\text{-}O_2)TMG_3tren]^+$ in solutions equilibrated with natural abundance O_2 (Figure 5). Measurements were performed by equilibrating samples at the experimental temperature and then isolating all of the O_2 from the copper-containing solutions. The yield of O_2 in these experiments was typically 97 ± 9% based upon the initial concentration of $[Cu(\eta^1\text{-}O_2)TMG_3tren]^+$ estimated from the NMR spectrum.

The measurements of ^{18}O EIEs rely upon precise determination of O_2 pressure changes and the ^{18}O:^{16}O ratios (cf. eq 4). The error in the IRMS analysis is very small (±0.0002). More conservative error limits, reflecting the precision of all manipulations,[10] were estimated from repeated measurements upon solutions containing natural abundance O_2. Data collected between 213 and 273 K indicate an average ^{18}O EIE = 1.0148 ± 0.0012. This value is within the errors of the individual ^{18}O EIEs determined at the temperature extremes.

3.2. Density Functional Calculations. Optimized structures of $[Cu(\eta^1\text{-}O_2)TMG_3tren]^+$ were determined for the unrestricted triplet, restricted singlet, and unrestricted broken-symmetry states. Calculations assuming a restricted singlet state had previously been used to corroborate the assignment of the resonance Raman spectrum (see below).[16] Frequency calculations on the energy-minimized structures afforded several isotopically sensitive vibrations which were used in eqs 8−10 without scaling. The full sets of the calculated frequencies are provided in the Supporting Information.

The calculated energy of the triplet $[Cu(\eta^1\text{-}O_2)TMG_3tren]^+$ is 16.3 kcal mol^{-1} lower than that of the restricted singlet state and 7.3 kcal mol^{-1} lower than that of the broken-symmetry state. The biradical nature of a Cu(II) superoxide species makes the accurate calculation of the state-energy splitting quite difficult because the biradical singlet cannot be represented by a single Kohn−Sham determinant.[49−52] Therefore, while experiment clearly indicates the triplet to be dominant at the temperatures studied, it is unlikely that the DFT calculations provide a reliable, quantitative measure of that preference.

Calculations were performed on the compounds in Figure 6 for comparison to $[Cu(\eta^1\text{-}O_2)TMG_3tren]^+$. Relevant structural results are presented in Table 1 for the mixed and triplet states. The calculations indicate longer O−O bond distances and lower O−O stretching frequencies (ν_{O-O}) for the side-on structures relative to those of the end-on structures.[53] The results are arranged to reflect the extent of O−O reduction, with $[Cu(\eta^1$-

(48) (a) Rybak-Akimova, E. V.; Otto, W.; Deardorf, P.; Roesner, R.; Busch, D. H. *Inorg. Chem.* **1997**, *36*, 2746−2753. (b) Drago, R. S.; Cannady, J. P.; Leslie, K. A. *J. Am. Chem. Soc.* **1980**, *102*, 6014−6019. (c) Fry, H. C.; Scaltrito, D. V.; Karlin, K. D.; Meyer, G. *J. Am. Chem. Soc.* **2003**, *125*, 11866−11871.

(49) Gherman, B. F.; Cramer, C. J. *Inorg. Chem.* **2004**, *43*, 7281−7283.
(50) Aboelella, N. W.; Kryatov, S.; Gherman, B. F.; Brennessel, W. W.; Young, V. G.; Sarangi, R.; Rybak-Akimova, E.; Hodgson, K. O.; Hedman, B.; Solomon, E. I.; Cramer, C. J.; Tolman, W. B. *J. Am. Chem. Soc.* **2004**, *126*, 16896−16911.
(51) Gherman, B. F.; Heppner, D. E.; Tolman, W. B.; Cramer, C. J. *J. Biol. Inorg. Chem.* **2006**, *11*, 197−205.
(52) Kinsinger, C. R.; Gherman, B. F.; Gagliardi, L.; Cramer, C. J. *J. Biol. Inorg. Chem.* **2005**, *10*, 778−789.
(53) Cramer, C. J.; Tolman, W. B.; Theopold, K. H.; Rheingold, A. L. *Proc. Natl. Acad. Sci. U.S.A.* **2003**, *100*, 3635−3640.

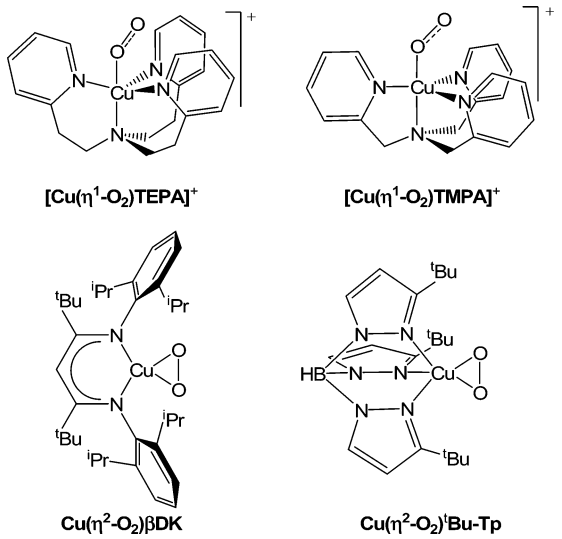

Figure 6. Mononuclear end-on (η^1) and side-on (η^2) CuO_2 complexes.

Table 1. Comparison of Calculated O−O Stretching Frequencies and Bond Lengths to the Available Experimental Data for Mononuclear CuO_2 Compounds

	ν_{O-O} ($\Delta^{16,18}$) (cm^{-1})		bond length (Å)	
	exp	calcd	exp	calcd
O_2[a]	1556.3(43.8)[b]	1550(44)	1.21[b]	1.22
$[Cu(\eta^1\text{-}O_2)TEPA]^+$[c]	n.d.	1279(29)	n.d.	1.27
$[Cu(\eta^1\text{-}O_2)TMPA]^+$[c]	n.d.	1251(33)	n.d.	1.28
$[Cu(\eta^1\text{-}O_2)TMG_3tren]^+$[a]	1117(28)[d]	1218(32)	1.28[e]	1.29
$Cu(\eta^2\text{-}O_2)$tBu-Tp[c]	1112(26)[f]	1124(31)	1.22[g]	1.33
$Cu(\eta^2\text{-}O_2)\beta$DK[c]	968(25)[h]	1013(28)	1.39[i]	1.38

[a] Unrestricted triplet calculation. [b] Reference 56. [c] Unrestricted singlet calculation. [d] Reference 16. [e] Reference 15. [f] Reference 21. [g] Reference 7a. [h] Reference 57. [i] Reference 7b.

$O_2)TMG_3tren]^+$ lying between the proposed[54] end-on compounds, $[Cu(\eta^1\text{-}O_2)TEPA]^+$ and $[Cu(\eta^1\text{-}O_2)TMPA]^+$, and the structurally characterized side-on species, $Cu(\eta^2\text{-}O_2)$-tBu-Tp and $Cu(\eta^2\text{-}O_2)\beta$DK.[7a,b]

In some cases, the experimental parameters differ significantly from the calculated ones. For example, the crystallographically determined bond length for a trispyrazolylborate $Cu(\eta^2\text{-}O_2)$ compound analogous to $Cu(\eta^2\text{-}O_2)$tBu-Tp is likely in error, owing to the librational motion of the O_2 fragment and an erroneously short, fitted bond length.[53] Another example involves $[Cu(\eta^1\text{-}O_2)TMG_3tren]^+$, which exhibits a ν_{O-O} in acetone solution that is $\sim$100 cm^{-1} less than the value calculated in the gas phase.

In the original report, close matching of the observed and calculated ν_{O-O} was reported for the restricted singlet structure of $[Cu(\eta^1\text{-}O_2)TMG_3tren]^+$.[16] While we have reproduced this calculation,[24] a revised treatment is clearly in order in view of the present results which establish that $[Cu(\eta^1\text{-}O_2)TMG_3tren]^+$ is paramagnetic.[55] The lack of agreement between the calculated and experimental stretching frequencies could, in principle, reflect enhancement of the ionic character within $[Cu(\eta^1\text{-}O_2)TMG_3tren]^+$ by the polar solvents. Although difficult to quantify, the increased charge transfer within $Cu^{II}-O_2^{-I}$ would be expected to lower the ν_{O-O} due to population of antibonding orbitals.

To probe the influence of solvent dielectric, we recomputed the frequencies for a triplet structure of $[Cu(\eta^1\text{-}O_2)TMG_3tren]^+$ reoptimized while including continuum acetone solvation effects within the polarized continuum model (PCM). Consistent with our hypothesis, the polar solvent enhanced charge transfer to O_2 which was manifested in an increased bond length (0.006 Å) and decreased stretching frequency (now 1183 cm^{-1} compared to 1218 cm^{-1} in the gas phase). While this does not completely resolve the difference between theory and experiment, it does substantially improve the agreement between the predicted O−O stretching frequency as well as the predicted EIE (vide infra). The remaining error might be associated with ion-pairing to the counterion, incompleteness of the one-particle basis set, and inaccuracy in the density functional.

Best agreement with the experimental EIE for $[Cu(\eta^1\text{-}O_2)TMG_3tren]^+$ is obtained using the frequencies obtained including the effects of continuum acetone solvation as shown in the Figure 5. Polarization effects associated with solvent are, to first order, proportional to $(1 - \epsilon^{-1})$ where ϵ is the dielectric constant of the solvent.[38] In the case of acetone, the value of $(1 - \epsilon^{-1})$ is 0.952. For DMF, the corresponding value is 0.974, which differs from acetone by about 2%.[43] Thus, insignificant changes in electronic structure would be expected between structures optimized in continuum models for these two solvents, and it is not surprising that there is good agreement between the computed and experimental EIEs.

3.3. Calculations of Oxygen Equilibrium Isotope Effects. ^{18}O EIEs were calculated at varying temperatures using eqs 7−10 which represent the gas-phase partition functions. The gas-phase vibrational frequencies for O_2 and the various oxygenated copper compounds were obtained from the density functional calculations described above. The *m*PWPW91 functional with the 6-311G* basis set on oxygen (previously used for other metal−O_2 complexes[52,53]) is particularly appropriate for this purpose as it reproduces the experimental O−O stretching frequency, isotope shift, and bond length of free O_2. Other methods (for example one employed by Popp et al. in a recent study of a palladium dioxygen complex[20b]) can fail in this respect, leading to potential errors in comparing experimental and theoretical isotope effects.

The maximum ^{18}O EIEs derived from calculations of isotopic partition functions at different temperatures are provided in Table 2. For $[Cu(\eta^1\text{-}O_2)TMG_3tren]^+$, the measured and calculated ^{18}O EIEs agree quite well even without the continuum dielectric correction. Use of the experimentally determined ν_{O-O} = 1556.3 cm^{-1} and $^{16,18}\Delta$ = 43.8 cm^{-1} for O_2[14,56] gave ^{18}O EIE_{calc} of 1.0125 which is quite close to the 1.0128 estimated from the ν_{O-O} = 1550 cm^{-1} and $^{16,18}\Delta$ = 44 cm^{-1} calculated for gas phase O_2 in this study. The ν_{O-O} calculated in acetone is 1537 cm^{-1} and $^{16,18}\Delta$ = 43 cm^{-1}. The use of unscaled values gives reasonably good agreement with the experimentally determined ^{18}O EIE = 1.0148.[58] Comparisons of the experimental to computational ^{18}O EIEs for the η^2-CuO_2 species in Figure 6 have not been possible due to the lack of reversibility in the reactions with O_2.

(54) Smirnov, V. V.; Roth, J. P. *J. Am. Chem. Soc.* **2006**, *128*, 3683−3695.
(55) Similar results have been obtained in magnetic circular dichroism studies (Schindler, S. Personal communication.) and will be the subject of a forthcoming manuscript.
(56) Chase, M. W., Jr.; Curnutt, J. L.; Downey, J. R., Jr.; McDonald, R. A.; Syverud, A. N.; Valenzuela, E. A. *J. Phys. Chem. Ref. Data* **1982**, *11*, 695−940.
(57) Spencer, D. J.; Aboelella, N. W.; Reynolds, A. M.; Holland, P. L.; Tolman, W. B. *J. Am. Chem. Soc.* **2002**, *124*, 2108−2109.

Table 2. Oxygen Equilibrium Isotope Effects (^{18}O EIE_{calc}) and Partition Functions Calculated from Eqs 7−11; Tabulated Values Correspond to the Temperatures at Which the Maximum ^{18}O EIEs Are Observed

	^{18}O EIE_{calc}	ZPE	EXC	MMI (eq 10)	MMI × EXC	MMI (eq 11)
$[(\eta^1\text{-}O_2)CuTEPA]^+$ [a]	1.0107[b]	0.9597	0.9192	1.1457	1.0531	1.1452
$[(\eta^1\text{-}O_2)CuTMPA]^+$ [a]	1.0128[c]	0.9644	0.9207	1.1406	1.0502	1.1420
$[(\eta^1\text{-}O_2)CuTMG_3tren]^+$ [d]	1.0129[b]	0.9589	0.9174	1.1515	1.0564	1.1509
$(\eta^2\text{-}O_2)Cu^tBu\text{-}Tp$[a]	1.0239[e]	0.9529	0.9367	1.1472	1.0746	1.1485
$(\eta^2\text{-}O_2)Cu\beta DK$[a]	1.0251[f]	0.9558	0.9337	1.1487	1.0725	1.1507

[a] Unrestricted singlet (mixed-state) calculation. [b] T_{max} = 243 K. [c] T_{max} = 222 K. [d] Unrestricted triplet calculation. [e] T_{max} =173 K. [f] T_{max} = 197 K.

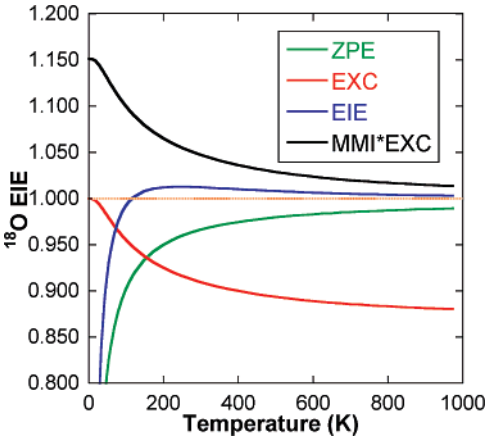

Figure 7. Calculation of the gas-phase partition functions and ^{18}O EIE upon formation of $[Cu(\eta^1\text{-}O_2)TMG_3tren]^+$ from $^{16,16}O_2$ and $^{16,18}O_2$.

The temperature dependences of the equilibrium isotope effects as well as the contributing isotopic partition functions were calculated to obtain insights as to the theoretical origins of the ^{18}O EIEs. The results obtained for $[Cu(\eta^1\text{-}O_2)TMG_3tren]^+$ are shown in Figure 7. The ^{18}O EIE_{calc} begins as an inverse value at the lowest temperatures and then passes through a normal maximum as the temperature increases. This is the result of a negative exponential relationship of the ZPE to temperature and the compensating influence of MMI × EXC. In all cases, the ^{18}O EIEs are predicted to be relatively insensitive to temperature over the experimentally accessible range. Similar results are indicated in the calculations using the polarized continuum model.[24] At the highest temperatures, the ^{18}O EIE_{calc} approaches unity as the inverse ZPE effect vanishes and EXC approaches 1/MMI.

The dependence of ^{18}O EIE_{calc} upon temperature is essentially the same for all of the CuO_2 compounds.[24] The enthalpic contribution to the isotope effect, represented by ZPE, is only slightly different for the η^1-species (0.9589−0.9644) and the η^2-species (0.9529, 0.9558). Similar behavior is indicated for the EXC terms: η^1-species (0.9174−0.9207) and η^2-species (0.9337, 0.9367). The temperature independent MMI terms are calculated to be large for both types of products, ranging from 1.1420 to 1.1509 without a discernible trend. The entropic contribution, EXC × MMI, apparently differentiates the end-on (1.0502−1.0564) from the side-on (1.0725, 1.0746) structures.

The temperature dependences of ^{18}O EIE_{calc} are also similar for the different electronic structures of $[Cu(\eta^1\text{-}O_2)TMG_3tren]^+$. For the triplet state, the ^{18}O EIE_{calc} passes through a maximum of 1.0128 at 243 K. For the mixed and singlet states, the maxima at 1.0134 and 1.0144 occur at 255 and 247 K, respectively.[19] The gas phase ν_{O-O} associated with these structures vary from 1218 cm^{-1} (triplet) to 1198 cm^{-1} (unrestricted singlet) to 1140 cm^{-1} (singlet).[24]

Discernible differences in the temperature dependences of the ^{18}O EIE_{calc} are predicted for the end-on and side-on structures. The maximum values predicted for $[Cu(\eta^1\text{-}O_2)TEPA]^+$ (1.0107) and $[Cu(\eta^1\text{-}O_2)TMPA]^+$ (1.0128) occur at 243 and 222 K, respectively, similar to that of $[Cu(\eta^1\text{-}O_2)TMG_3tren]^+$. In contrast, the maximum ^{18}O EIE_{calc} for $Cu(\eta^2\text{-}O_2)\text{-}^tBu\text{-}Tp$ (1.0239) and $Cu(\eta^2\text{-}O_2)\beta dk$ (1.0251) are at 173 and 197 K. The observation that the maximum isotope effects occur at lower temperatures for the side-on structures than for the end-on structures is consistent with a less significant contribution to the ^{18}O EIE from the low-frequency modes. For example in the case of the triplet structure for $[Cu(\eta^1\text{-}O_2)TMG_3tren]^+$, truncating the set of frequencies such that only vibrations above 100 cm^{-1} are used in the calculations, results in a slight change in the isotope effect from 1.0129 to 1.0136 and shifting of the maximum from 243 to 231 K.

4. Discussion

Ever since Pauling's assignment of oxyhemoglobin as an end-on ferrous dioxygen adduct ($Fe^{II}-O_2^0$),[1a] the electronic structures of metal-bound dioxygen species have been subject to debate.[1a,6a,17−19,59−63] Studies of the cobalt-reconstituted proteins have provided perhaps the most compelling experimental support for the alternative ferric superoxide ($Fe^{III}-O_2^{-I}$) description of oxyhemoglobin and related systems.[59−61] Electron paramagnetic resonance (EPR) spectroscopy has elegantly been applied to assess the degree of internal electron transfer and, hence, the valence bond contributions to transition-metal-activated oxygen structures.[62] The EPR analysis has largely been limited to O_2 adducts of cobalt where nuclear hyperfine interactions are observed between the unpaired electron and the ^{59}Co- or ^{17}O-labeled oxygen.[59,60,63]

(58) While the analysis of EIEs using scaled quantum mechanical force constants may seem to be a more rigorous approach for comparing theory to experiment, such a procedure would require a large number of experimental data, including several vibrational frequencies for each of the isotopologues, in order to scale a reasonable portion of the quantum mechanical Hessian matrix.

(59) (a) Hoffman, B. M.; Petering, D. H. *Proc. Natl. Acad. Sci. U.S.A.* **1970**, *67*, 637−643. (b) Jones, R. D.; Summervill, D. A.; Basolo, F. *Chem. Rev.* **1979**, *79*, 139−179.
(60) (a) Ikeda-Saito, M.; Horui, H.; Inubushi, T.; Yonetani, T. *J. Biol. Chem.* **1981**, *256*, 10267−10271 and refs therein. (b) Gupta, R. K.; Mildvan, A. S.; Yonetani, Takashi; Srivastava, T. S. *Biochem. Biophys. Res. Commun.* **1975**, *67*, 1005−1012.
(61) Lever, A. B. P.; Ozin, G. A.; Gray, H. B. *Inorg. Chem.* **1980**, *19*, 1823−1824.
(62) (a) Herman, Z. S.; Loew, G. H. *J. Am Chem. Soc.* **1980**, *102*, 1815−1821. (b) Jensen, K. P.; Ryde, U. *J. Biol. Chem.* **2004**, *279*, 14561−14569. (c) Jensen, K. P.; Roos, B. J.; Ryde, U. *J. Inorg. Biochem.* **2005**, *99*, 45−54. (d) Jensen, K. P.; Roos, B. J.; Ryde, U. *J. Inorg. Biochem.* **2005**, *99*, 978.
(63) (a) Tovrog, B. S.; Kitko, D. J.; Drago, R. S. *J. Am. Chem. Soc.* **1976**, *98*, 5144−5153. (b) Hoffman, B. M.; Szymanski, T.; Brown, T. G.; Basolo, F. G. *J. Am. Chem. Soc.* **1978**, *100*, 7523−7259. (c) Drago, R. S.; Corden, B. B. *Acc. Chem. Res.* **1980**, *13*, 353−360.

Formal oxidation-state assignments de-emphasize the importance of both ionic and covalent character within the bonds of various types of metal−dioxygen species.[61] The ^{18}O EIEs determined here for CuO_2 species, together with those determined previously for group IX transition metals, provide experimental support for a bonding continuum, from dioxygen to superoxide to peroxide-like structures.[6a,7c,49,53,54] It is interesting to consider how differing extents of ionic and covalent bonding influence reactivity. For example, the stable iron−oxygen adducts derived from O_2-transport and O_2-sensing heme proteins are known to dissociate $O_2^{\bullet-}$.[64] In contrast, the mononuclear non-heme iron- and copper active sites appear more likely to generate high-energy oxygen adducts that readily dissociate O_2. This is but one reason why such species can be difficult to detect spectroscopically.[65,66] In the enzymes, the kinetics of O_2 binding and subsequent substrate oxidation must be finely tuned to prevent oxidative damage to the surrounding protein.[67] The oxygen isotope effects provide a way to identify catalytic intermediates, which may be spectroscopically undetectable, and to correlate the vibrational structures of these species to reactivity.

The combined use of experiment and theory, as described in this work, has for many years been the cornerstone of isotope effect studies, with a significant portion of this work employing heavy atom isotope fractionation methods.[68−71] We add that the comparison of experimental to predicted oxygen isotope effects upon reactions of O_2 has been limited to but a few examples.[13a,69h,72,73]

4.1. Electronic Structures of End-on CuO_2 Species. [Cu(η^1-O_2)TMG_3tren]$^+$ exhibits an electronic structure that is different from those proposed for most other types of metal−oxygen adducts,[17−21,57] including those derived from heme.[59,62] That [Cu(η^1-O_2)TMG_3tren]$^+$ does not exhibit an X-band EPR spectrum is consistent with the compound having either a triplet or singlet structure. The paramagnetic NMR spectrum, together with the solution magnetic susceptibility, provides evidence for the former at least under the experimental conditions. The presence of two unpaired spins is most readily attributed to ferromagnetic coupling of an electron associated with copper(II) and another associated with the superoxide (O_2^{-I}) ligand. As mentioned above, another possibility could involve copper(I) bound to O_2^0 containing two unpaired electrons of the same spin.

The thermal instability of the isolated compound has unfortunately precluded magnetic susceptibility measurements in the crystalline state.[46] The characterization of the O_2 binding equilibria reported in this work can, however, provide a basis for future investigations of the magnetic properties.[55]

The paramagnetic [Cu(η^1-O_2)TMG_3tren]$^+$ exhibits a dominant contribution from the ionic ($Cu^{II}-O_2^{-I}$) structure, as indicated by the magnitude of the ^{18}O EIE (see below). Evidence for a tightly bound, inner-sphere complex rather than a weak association complex of [$Cu^{II}TMG_3$tren]$^{2+}$ and $O_2^{\bullet-}$ comes from the following observations: (i) [$Cu^{I}TMG_3$tren]$^{1+}$ is regenerated in 94 ± 6% yield upon removal of O_2 from a sample of [Cu(η^1-O_2)TMG_3tren]$^+$, (ii) no NMR spectral change is detected upon addition of [$Cu^{II}TMG_3$tren]$^{2+}$ to samples of either [$Cu^{I}TMG_3$tren]$^{1+}$ or [Cu(η^1-O_2)TMG_3tren]$^+$, and (iii) no EPR signal due to [Cu(η^1-O_2)TMG_3tren]$^+$ is observable at X-band frequency, under conditions where [$Cu^{II}TMG_3$tren]$^{2+}$ is readily quantified. The very favorable electrostatic interaction energy estimated for [$Cu^{II}TMG_3$tren]$^{2+}$ and $O_2^{\bullet-}$ ($\Delta G^\circ_{298K} = -21$ kcal mol^{-1}) from the redox potentials[15,74] and the calculated K_{O2} further argues against an outer-sphere complex.[75]

Qualitatively, the paramagnetism of [Cu(η^1-O_2)TMG_3tren]$^+$ could partly be attributable to the η^1 versus η^2 coordination and partly to the weak electron-donating nature of the ligand relative to those of the anionic Tp and βDK ligands. These features effectively eliminate the singlet copper(III) peroxide dianion character in the valence bond description of the compound. Calculations have predicted that end-on coordination substantially reduces the stability of the singlet relative to that of the triplet state in CuO_2 species, irrespective of ligand,[50−52] and have established that the ligands of lesser electron-donating ability stabilize end-on structures relative to side-on structures.[76]

Within the context of the density functional calculations, ferromagnetic coupling suggests decreased covalency within the Cu/O_2 interaction. This diminished covalency would more likely be the case for end-on oxygen adducts than for a side-on species. Ground-state singlet structures have been reported for

(64) (a) Gilles-Gonzalez, M. A.; Gonzalez, G.; Perutz, M. F.; Kiger, L.; Marden, M. C.; Poyart, C. *Biochemistry* **1994**, *33*, 8067−8073. (b) Gonzalez, G.; Gilles-Gonzalez, M. A.; Rybak-Akimova, E. V.; Buchalova, M.; Busch, D. H. *Biochemistry* **1998**, *37*, 10188−10194. (c) Shikama, K. *Chem. Rev.* **1998**, *98*, 1357−1373.

(65) For a possible exception of a stable FeO_2 species in a non-heme iron enzyme see: Brown, C. D.; Neidig, M. L.; Neibergall, M. B.; Lipscomb, J. D.; Solomon, E. I. *J. Am. Chem. Soc.* **2007**, *129*, 7427−7438 and refs therein.

(66) High-energy, end-on dioxygen adducts have also been proposed to form at diiron active sites. See: Wei, P.; Skulan, A. J.; Wade, H.; DeGrado, W. F.; Solomon, E. I. *J. Am. Chem. Soc.* **2005**, *127*, 16098−16106.

(67) Klinman, J. P. *Acc. Chem. Res.* **2007**, *40*, 325−333.

(68) Two historical overviews are provided by Bigeleisen, J.; Wolfsberg, M. In *Isotope Effects in Chemistry and Biology*; Kohen, A., Limbach, H. H., Eds.; CRC Press: Boca Raton, 2006; pp 1−39, 89−117.

(69) For examples related to reactions of O_2 see: (a) Nahm, K.; Li, Y.; Evanseck, J. D.; Houk, K. N.; Foote, C. S. *J. Am. Chem. Soc.* **1993**, *115*, 4879−4884. (b) Burger, R. M.; Tian, G.; Drlica, K. *J. Am. Chem. Soc.* **1995**, *117*, 1167−1168. (c) Andrews, L.; Chertihin, G. V.; Ricca, A.; Bauschlicher, C. W., Jr. *J. Am. Chem. Soc.* **1996**, *118*, 467−470. (d) Danset, D.; Manceron, L.; Andrews, L. *J. Phys. Chem. A* **2001**, *105*, 7205−7210. (e) Palmer, A. E.; Lee, S. K.; Solomon, E. I. *J. Am. Chem. Soc.* **2001**, *123*, 6591−6599. (f) Singleton, D. A; Hang, C.; Szymanski, M. J.; Meyer, M. P.; Leach, A. G.; Kuwata, K. T.; Chen, J. S.; Greer, A.; Foote, C.S.; Houk, K. N. *J. Am. Chem. Soc.* **2003**, *125*, 1319−1328. (g) Smirnov, V. V.; Roth, J. P. *J. Am. Chem. Soc.* **2006**, *128*, 16424−16425.

(70) For relevant studies of equilibrium isotope effects see: (a) Saunders, M.; Laidig, K. E.; Wolfsberg, M. *J. Am. Chem. Soc.* **1989**, *111*, 8889−8994. (b) Bender, B. *J. Am. Chem. Soc.* **1995**, *117*, 11239−11246. (c) Slaughter, L. M.; Wolczanski, P. T.; Klinckman, T. R. Cundari, T. R. *J. Am. Chem. Soc.* **2000**, *122*, 7953−7975. (d) Abu-Hasanayn, F.; Goldman, A. S.; Krogh-Jesperson, K. *J. Phys. Chem.* **1993**, *97*, 5890−5896.

(71) For several leading examples of combined experimental/computational methods for the determination of kinetic isotope effects on organic reactions, see: (a) Ralph, E. C.; Hirschi, J. S.; Anderson, M. A.; Cleland, W. W.; Singleton, D. A.; Fitzpatrick, P. F. *Biochemistry* **2007**, *46*, 7655−7664. (b) Gustin, D. J.; Mattei, P.; Kast, P.; Wiest, O.; Lee, L.; Cleland, W. W.; Hilvert, D. *J. Am. Chem. Soc.* **1999**, *121*, 1756−1757. (c) Meyer, M. P.; DelMonte, A. J.; Singleton, D. A. *J. Am. Chem. Soc.* **1999**, *121*, 10865−10874. (d) DelMonte, A. J.; Haller, J.; Houk, K. N.; Sharpless, K. B.; Singleton, D. A.; Strassner, T.; Thomas, A. A. *J. Am. Chem. Soc.* **1997**, *119*, 9907−9908. (e) Beno, B.R.; Houk, K. N.; Singleton, D. A. *J. Am. Chem. Soc.* **1996**, *118*, 9984−9985.

(72) (a) Roth, J. P.; Wincek, R.; Nodet, G.; Edmondson, D. E.; McIntire, W. S.; Klinman, J. P. *J. Am. Chem. Soc.* **2004**, *126*, 15120−15131. (b) References 13a, 13b, and 54 describe measured and calculated oxygen isotope effects on O_2 binding to transition metal compounds.

(73) Reference 20b describes what may be one of the first uses of density functional methods to calculate oxygen isotope effects relevant to those measured in refs 13a and 13b. There is disagreement between the experimental and calculated values for reasons that are not yet understood.

(74) Using $E_{1/2} = 0.26$ V versus NHE for [Cu(TMG_3Tren]$^{2+/1+}$ in acetone (ref 15) and $E_{1/2} = -0.62$ V versus NHE for O_2 in DMF, as quoted in Sawyer, D. T.; Sobkowiak, A.; Roberts, J. L., Jr. *Electrochemistry for Chemists*, 2nd ed.; Wiley: New York, 1995; pp 364−372.

(75) Slightly larger values have been estimated for $Co-O_2$ complexes. See: Taube, H. *Prog. Inorg. Chem.* **1986**, *34*, 607−625.

(76) Heppner, D. E.; Gherman, B. F.; Tolman, W. B.; Cramer, C. J. *Dalton Trans.* **2006**, 4773−4782.

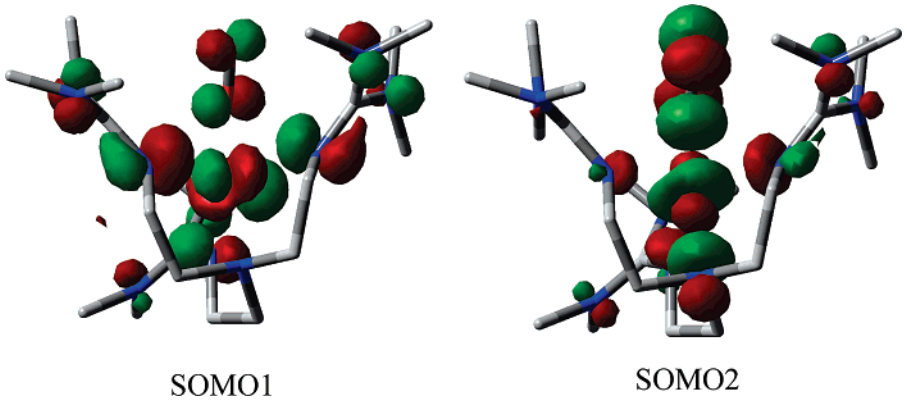

Figure 8. Singly occupied molecular orbitals (SOMOs) for the calculated triplet ground state of $[Cu(\eta^1\text{-}O_2)TMG_3tren]^+$. See the text for descriptions.

$Cu(\eta^2\text{-}O_2)^tBu\text{-}Tp$ and $Cu(\eta^2\text{-}O_2)\beta Dk$.[21,49,77] The magnetic properties of the proposed[54] $[Cu(\eta^1\text{-}O_2)TMPA]^+$ and its dimethylamino derivative[7h] have yet to be evaluated and should provide interesting comparisons to $[Cu(\eta^1\text{-}O_2)TMG_3tren]^+$ due to the isostructural nature of the compounds.[7d]

The calculations performed on $[Cu(\eta^1\text{-}O_2)TMG_3tren]^+$ discussed in Results (section 3.2.) suggest a large singlet vs triplet gap (ca. 10 kcal mol^{-1}). A full theoretical analysis of this $Cu-O_2$ system will be the subject of a forthcoming study.[78] Here we suggest simply that the triplet ground state can be attributed to a relatively weak interaction between the filled d_{z^2} orbital on copper and the singly occupied π^* molecular orbital on dioxygen with which it overlaps, possibly because of energy mismatch resulting from the geometric constraints and the weak electron-donating ability of the TMG_3tren ligand. Splitting of the O_2 π^* levels due to hybridization of one of these orbitals with the d_{z^2} is apparently too weak to overcome the exchange energy required to pair the electrons in the lower-energy noninteracting O_2 π^*.

Given such limited hybridization, the DFT calculations suggest that the complex has $Cu^I-O_2^0$ character. The covalency of the Cu−O interaction must, however, permit some charge transfer to the O_2 fragment with concomitant buildup of ferromagnetically coupled spin within the $Cu^{II}-O_2^{-I}$ species. This description is fully consistent with the solution magnetic susceptibility measurements presented herein, the previously reported O−O stretching frequency and bond distances which are intermediate of O_2 and $O_2^{\bullet-}$,[15,16] as well as the optical spectrum which shows a strong band ca. 440 nm typically assigned as a ligand to metal charge transfer.[6b,7d,16]

The two singly occupied molecular orbitals (SOMOs, see Figure 8) are consistent with this analysis. The lower-lying SOMO1 would ideally be associated with the noninteracting π^* orbital of O_2. The additional contributions from the TMG_3-tren ligand and the Cu d_{xy} orbitals are commonly observed for molecules of this size. The higher-energy SOMO2 is the hybrid $\pi^*-d_{z^2}$ orbital, also with additional contributions from the TMG_3tren ligand, especially the tertiary amine *trans* to the dioxygen ligand. A Mulliken analysis of the spin distribution for the structure computed including solvation effects places 1.38 units of spin on the O_2 fragment and the remaining 0.62 units on the Cu and coordinating N atoms, reflecting the degree of charge transfer associated with covalent bonding between the Cu and O_2.

Few transition-metal compounds have been reported to exhibit ground-state triplet electronic structures. A recent example[79] is a copper(II) compound containing an arylnitroxyl ligand. This species exists predominantly in the triplet state at temperatures between 100 and 300 K. The preference for the triplet electronic structure has been suggested to arise from the high-spin density on the nitroxyl, orthogonal (in the geometric sense) to the orbital containing the unpaired electron on copper. The computational results for $[Cu(\eta^1\text{-}O_2)TMG_3tren]^+$ raise the possibility that orbital orthogonality may not be a requirement for observable ferromagnetic coupling, given that this is the origin of the observed paramagnetism in the present study. In support of the calculations described in this work, "spin-flip" time-dependent density functional calculations have also predicted triplet ground states for CuO_2 compounds structurally related to $[Cu(\eta^1\text{-}O_2)TMG_3tren]^+$.[17a]

4.2. Interpretation of Equilibrium Isotope Effects. 4.2.1. Vibrational Structures of End-on and Side-on CuO_2 Species. The first ^{18}O equilibrium isotope effects upon the formation of mononuclear CuO_2 complexes from natural abundance O_2 have been determined. The O_2 is bound in an end-on manner in the one case where isotope effects can be both measured and calculated. The structure of $[Cu(\eta^1\text{-}O_2)TMG_3tren]^+$ may be analogous to those of intermediates proposed to effect C−H oxidation in enzymes.[4,5] In such instances, competitive ^{18}O kinetic isotope effects have been suggested as evidence that the CuO_2 species is the reactive oxidant.[11,12] The rigorous application of ^{18}O isotope effects to the identification of such intermediates has been limited, however, due to the absence of benchmarks and computational methods for predicting activated oxygen structures at the requisite level of detail.

Interestingly, the ^{18}O EIE of 1.0148 which characterizes $[Cu(\eta^1\text{-}O_2)TMG_3tren]^+$ is significantly larger than those seen for other end-on oxygen adducts. Small ^{18}O EIEs (1.0041−1.0066) have been reported for O_2 binding to hemes[14] as well as for synthetic cobalt compounds.[13a] Meanwhile, the isotope effect for $[Cu(\eta^1\text{-}O_2)TMG_3tren]^+$ is significantly smaller than the ^{18}O EIEs calculated for side-on CuO_2 compounds (1.024, 1.025) as well as those measured for side-on peroxide compounds of other

(77) Reynolds, A. M.; Gherman, B. F.; Cramer, C. J.; Tolman, W. B. *Inorg. Chem.* **2005**, *44*, 6989−6997. Sarangi, R.; Aboelella, N.; Fujisawa, K.; Tolman, W. B.; Hedman, B.; Hodgson, K. O.; Solomon, E. I. *J. Am. Chem. Soc.* **2006**, *128*, 8286−8296.

(78) Cramer, C. J.; Gour, J. R.; Wloch, M.; Piecuch, P.; Rehaman Moughal Shahi, A.; Gagliardi, L. Manuscript in preparation.

(79) Osanai, K.; Okazawa, A.; Nogami, T.; Ishida, T. *J. Am. Chem. Soc.* **2006**, *128*, 14008−14009.

transition metals (1.020−1.028). These results support a continuum bonding description where the extent of O−O reduction is correlated to, yet does not alone determine, the magnitude of the ^{18}O EIE. We have now confirmed that measured ^{18}O EIEs can be reproduced using vibrational frequencies obtained from the appropriate density functional methods.

4.2.2. Physical Origins of the Isotope Effects. Analysis of isotopic stretching frequencies within the formalism of Bigeleisen and Goeppert-Mayer provides valuable insights concerning the origins of ^{18}O EIEs upon O_2 binding to reduced metal centers. We have performed calculations of isotope-dependent partition functions at different temperatures to determine how enthalpy and entropy contribute to the ^{18}O EIEs.

The coordination of O_2 is entropically unfavorable but enthalpically driven by the formation of metal−O bonds, at the expense of weakening the O−O bond. Extensive enthalpy−entropy compensation is expected for O_2 binding to transition metals because of the low-frequency vibrational modes created which connect the isotopic sites within the products.[80] Similar behaviors have been reported by Parkin and co-workers to characterize the formation of organometallic σ complexes of H_2 and CH_4. Unlike O_2, in these examples, the bound substrates are not believed to undergo extensive reduction.[81]

The isotopic partition functions in Table 2 would seem to suggest that the primary contribution to the ^{18}O EIE is entropic (EXC × MMI) rather than enthalpic (ZPE) in origin; however, this is not meant to suggest that changes in force constants are unimportant.[68] In all of the reactions analyzed, the ZPE terms are inverse and span a relatively narrow range (0.953−0.964). This observation argues against a dominant contribution from reduction of the O−O bond, as assumed in an earlier model;[14] in this case the accompanying change in force constant would result in a normal (>1) effect.

The inverse ZPE terms indicate a net increase in bonding within the product relative to free O_2. This observation is consistent with the favorable $\Delta H = -8.4$ kcal mol^{-1} determined for the formation of $[Cu(\eta^1\text{-}O_2)TMG_3tren]^+$. The absence of a trend among the ZPE terms for η^1- and η^2-O_2 structures implies that strengthening of the Cu−O bond results in a commensurate weakening of the O−O bond and *vice versa*. In support of this view, similar *ZPE* terms have been estimated for the formally η^1-superoxide and η^2-peroxide compounds derived from group IX transition metals.[82]

The entropic contribution to the isotope effect, EXC × MMI, reflects the mass-dependent population difference arising from rotations and translations of free O_2 which are converted to low-frequency vibrations within the product. Large normal MMI terms (1.14−1.15) are calculated representing the loss of mass discrimination among translational and rotational modes in free O_2 upon its coordination to the heavy metal fragment. The MMI terms are offset by inverse EXC terms (0.9174−0.9367) originating from the increased number of vibrational modes within the product. The thermal population of these modes is greater for the heavier isotopologue than for the lighter one due to the more closely spaced energy levels.

In contrast to the ZPE effect, the EXC × MMI appears to differentiate the two classes of CuO_2 adducts: η^1 (1.0502−1.0564) and η^2 (1.0725, 1.0746). Similar differences have also been calculated for the η^1-superoxide and η^2-peroxide structures derived from group IX transition metals;[82] except in the case of the $Co(\eta^1\text{-}O_2)$ structures the EXC × MMI terms are somewhat smaller than for the $Cu(\eta^1\text{-}O_2)$ structures. In future studies, we will attempt to experimentally delineate the enthalpic and entropic contributions by examining the temperature dependence of the isotope effects over ranges where they are predicted to vary significantly and the ZPE terms are predicted to transition from normal to inverse.[82]

4.3. Implications for Enzymatic O_2 Activation. The ^{18}O EIEs in the present study provide boundary conditions for the interpretation of ^{18}O KIEs upon enzymatic reactions.[4,10−12,23,69g] By virtue of being competitive measurements, the latter probe all steps beginning with the association of the enzyme and O_2 up to and including the first kinetically irreversible step. The ^{18}O EIE is often assumed to define the upper limit to the ^{18}O KIE for a reaction involving a single, irreversible step. This relationship, which derives from Transition State Theory and the formulation of the reaction coordinate as classical with a transition state that has a vibrational structure intermediate between the reactant and the product, has not yet been rigorously tested. This assumption has, however, served as the basis for interpreting heavy atom kinetic isotope effects for many years.[83] Nevertheless, the isotope effects described in this study are recommended as benchmarks for the characterization of intermediates formed in the pre-equilibrium steps of O_2 reduction mechanisms.

4.3.1. Copper Monooxygenases. Dopamine β-monooxygenase (DβM) and peptidylglycine α-hydroxylating monooxygenase (PHM) are structurally homologous enzymes which activate O_2 for the biosynthesis of hormones and neurotransmitters. An outstanding question has been the identity of the species responsible for substrate C−H oxidation by H• abstraction.[4,5,84] The remarkably similar ^{18}O KIEs determined for the enzyme reactions have been cited as evidence that a copper species, with an intact O−O bond, is the active oxidant. A copper(II) superoxide species has been proposed on the basis of observations with deuterium-labeled substrates[4] where ^{18}O KIEs vary from 1.0197 ± 0.0003 to 1.0256 ± 0.0003 in DβM and from 1.0173 ± 0.0009 to 1.0212 ± 0.0018 in PHM upon replacing ^1H with ^2H at the reactive position.

The ^{18}O EIE determined for $[Cu(\eta^1\text{-}O_2)TMG_3tren]^+$ (1.0148) is consistent with the proposal of the pre-equilibrium formation of the copper(II) end-on superoxide intermediate in DβM and PHM.[85] The side-on structure[5] cannot be rigorously excluded, however, since the ^{18}O EIEs for $Cu(\eta^2\text{-}O_2)^tBu\text{-}Tp$ and $Cu(\eta^2\text{-}O_2)\beta DK$ are close to the upper limits defined by the range of KIEs. A slight increase in the ^{18}O KIE observed for the enzyme reaction relative to the ^{18}O EIE is anticipated due to

(80) Huskey, W. P. In *Enzyme Mechanism from Isotope Effects*; Cook, P. F., Ed.; CRC Press: Boca Raton, 1991 pp 37−72.
(81) (a) Janak, K. E.; Parkin, G. *J. Am. Chem. Soc.* **2003**, *125*, 13219−13224. (b) Janak, K. E.; Parkin, G. *J. Am. Chem. Soc.* **2003**, *125*, 6889−6891.
(82) Lanci, M. P.; Smirnov, V. V.; Roth, J. P. Manuscript in preparation.
(83) The heart of the issue is the reaction coordinate frequency and its isotope sensitivity. The assumptions with respect to heavy atom kinetic isotope effects upon O_2 binding are discussed in refs 11, 13b, 68 pp 18−25, ref 80 pp 44−47, and in the classic monograph: Melander, L.; Saunders, W. H., Jr. *Reaction Rates of Isotopic Molecules*; Wiley: New York, 1980; pp 45−49, 64−83, 272−275.
(84) Crespo, A.; Marti, M. A.; Roitberg, A. E.; Amzel, L. M.; Estrin, D. A. *J. Am. Chem. Soc.* **2006**, *128*, 12817−12828.
(85) The end-on geometry has also been supported by recent density functional calculations in ref 49.

the subsequent step where the O−O bond is reduced further upon H• transfer.

4.3.2. Copper Amine Oxidases. The ^{18}O EIE determined for $[Cu(\eta^1\text{-}O_2)TMG_3tren]^+$ is also relevant to the mechanism by which copper- and topaquinone(TPQ)-containing amine oxidases reduce O_2 to H_2O_2. This reaction, in structurally homologous enzymes from a variety of sources, provides the oxidizing equivalents needed to convert primary amines to aldehydes. Two proposals which differ with respect to the role of the copper in activating O_2 have been considered.[86] Dooley and co-workers originally proposed that O_2 binds to copper(I) in the initial step of O_2 reduction. Klinman and co-workers have put forth an alternative mechanism where O_2 reacts directly with $TPQ_{reduced}$ by outer-sphere electron transfer.[23b,87]

The ^{18}O KIEs determined for copper amine oxidases have been difficult to interpret in the absence of boundary conditions for structurally defined CuO_2 species. The ^{18}O KIEs reported for the enzymes from yeast and from bovine serum range from 1.008 to 1.011,[23b,87a,88] well outside the limits expected for outer-sphere electron transfer.[11,12,69g,72a]

Larger ^{18}O KIEs from 1.014 to 1.018 have recently been determined for the amine oxidases from pea seedling and *Arthrobacter globiformis*.[89] That these values are close to the ^{18}O EIE determined for $[Cu(\eta^1\text{-}O_2)TMG_3tren]^+$ raises the possibility that a copper(II) superoxide species is formed in a pre-equilibrium step. Thus, the electron transfer from TPQsemiquinone to $Cu(\eta^1\text{-}O_2)$ may be rate-determining in the reaction of copper amine oxidases with O_2.[12] Such a mechanism, involving reversible O_2 binding prior to electron or coupled electron/proton transfer to CuO_2, is similar to that proposed for the copper monooxygenases. The observation in the yeast and bovine amine oxidase, where the ^{18}O KIE is somewhat smaller than the expected ^{18}O EIE, further implies an internal commitment factor, where formation of the $Cu(\eta^1\text{-}O_2)$ species contributes to the rate-limiting step.[12,90]

5. Conclusions

On the basis of oxygen isotope effect measurements together with density functional methods we have outlined a new approach to characterizing unstable O_2-derived species. Proof-of-principle is provided by (i) the demonstration that the calculated and observed oxygen equilibrium isotope effects are in good agreement for $[Cu(\eta^1\text{-}O_2)TMG_3tren]^+$ and (ii) comparisons of calculated values which reveal a trend where the ^{18}O EIEs increase in direct proportion to the level of O−O reduction, from oxygen-like to superoxide-like to peroxide-like structures.

The first competitive isotope effects upon reversible O_2 binding to form a structurally defined CuO_2 species have been determined. Interestingly, the ^{18}O EIE upon $[Cu(\eta^1\text{-}O_2)TMG_3tren]^+$ formation is significantly larger than those measured for structurally analogous end-on oxygen adducts derived from iron and cobalt. Analysis within the context of the accepted theory implies differences in the low-frequency stretching modes which characterize the metal−oxygen interaction. The elevated isotope effect suggests increased ionic character within the valence bond description. Precisely how this relates to the finding that $[Cu(\eta^1\text{-}O_2)TMG_3tren]^+$ is paramagnetic is not yet understood; however, density functional calculations suggest a triplet ground state due to the lack of significant interaction between the d_{z^2} orbital on copper and the π^* orbitals on dioxygen.

The agreement observed between the measured and calculated isotope effects for $[Cu(\eta^1\text{-}O_2)TMG_3tren]^+$ validates the application of the theoretical formalism and density functional methods to calculating oxygen isotope effects for ground-state, metal-activated oxygen structures. The importance of using the appropriate functional and basis set cannot be overemphasized since the isotope effects are very sensitive to small frequency shifts. Validating the quantitative utility of such calculations is a vital step toward applying DFT to predict transition-state structures and the accompanying kinetic isotope effects upon enzymatic oxidation reactions.

Analyzing the isotope effects in light of the constituent isotopic partition functions has provided new insights concerning the physical origins. Calculations at varying temperatures reveal extensive enthalpy−entropy compensation; this can be understood in terms of the binding of O_2 concomitant with the formation of new isotopically sensitive low-frequency modes unique to the product. An isotope effect is thus observed to be characteristic of the dioxygen-, superoxide-, or peroxide-like structure. This view is in contrast to an earlier model where the isotope effect was assumed to arise primarily from the change in the O−O force constant. While this is most certainly a contributing factor to the observed trends, its influence cannot be deconvolved from that of the new metal−oxygen bonds formed.

The results described above have important implications for interpreting isotope effects upon oxidation reactions, particularly when O_2 is activated by inner-sphere electron transfer. In these cases, the oxygen EIEs for structurally defined compounds provide relevant benchmarks for identifying O_2-derived intermediates during enzyme catalysis.

Acknowledgment. We acknowledge funding provided by a Martin and Mary Kilpatrick Fellowship (M.P.L.), the National Science Foundation: CAREER award CHE-0449900 (J.P.R) and CHE-0610183 (C.J.C.), the Research Corporation Cottrell Scholar Award CS1461 (J.P.R.) and the Alfred P. Sloan Foundation (J.P.R.). We thank Dr. Charles A. Long for technical support and Siegfried Schindler and Jim Mayer for helpful discussions.

Supporting Information Available: Additional synthetic and procedural details, spectroscopic results, stretching frequencies from density functional calculations, graphs showing the calculated temperature dependence of oxygen isotope effects, and a full list of authors for ref 42. This material is available free of charge via the Internet at http://pubs.acs.org.

JA074620C

(86) Juda, G. A.; Shepard, E. M.; Elmore, B. O.; Dooley, D. M. *Biochemistry* **2006**, *45*, 8788−8800.
(87) (a) Mills, S. A.; Goto, Y.; Su, Q.; Plastino, J.; Klinman, J. P. *Biochemistry* **2002**, *41*, 10577−10584. (b) Takahashi, K.; Klinman, J. P. *Biochemistry* **2006**, *45*, 4683−4694.
(88) Su, Q.; Klinman, J. P. *Biochemistry* **1998**, *37*, 12513−12525.
(89) Mukherjee, A.; Lanci, M. P.; Brown, D. E.; Shepard, E. M.; Dooley, D. M.; Roth, J. P. Manuscript in preparation.
(90) Welford, R. W. D.; Lam, A.; Mirica, L. M.; Klinman, J. P. *Biochemistry* **2007**, *46*, 10817−10827.